Supplementary Data

Design, Synthesis and Anti-mycobacterial Evaluation of Imidazo-[1,2-a]-pyridine analogues

Yogesh Mahadu Khetmalis[a], Surendar Chitti[a], Anjani Umarani Wunnava[b], Banoth Karan Kumar[c], Muthyala Murali Krishna Kumar[b], Sankaranarayanan Murugesan[c], Kondapalli Venkata Gowri Chandra Sekhar*[a]

[a]*Department of Chemistry, Birla Institute of Technology and Science, Pilani, Hyderabad Campus, Jawahar Nagar, Hyderabad 500 078, Telangana, India*

[b]*College of Pharmaceutical Sciences, Andhra University, Visakhapatnam, Andhra Pradesh – 530 003, India*

[c]*Medicinal Chemistry Research Laboratory, Department of Pharmacy, Birla Institute of Technology and Science, Pilani, 333031, India*

Table of Contents **Page No.**

*Corresponding author

Tel.:+91 40 66303527; E-mail: kvgc@hyderabad.bits-pilani.ac.in; kvgcs.bits@gmail.com

Experimental

Chemistry

All the reagents were procured from commercial available sources and used with further purification wherever necessary. All reactions were monitored by thin layer chromatography (TLC) performed on E-Merck 0.25 mm pre-coated silica gel aluminum plates (60 F254) using mixture of pet ether and ethyl acetate. Visualization of the spots on TLC was achieved by exposure to UV light. Column chromatography was performed using silica gel (Acme, 100-200mesh). Solvents were dried and purified by distillation prior to use. Solvents for chromatography (pet ether and ethyl acetate) were distilled prior to use. Evaporations were carried out under reduced pressure on Heidolf rotary evaporator. ^{1}H and ^{13}C NMR spectra were recorded on Bruker (400 MHz for ^{1}H, 100 MHz for ^{13}C), in MeOH-d_4 or DMSO-d_6. Chemical shifts have been expressed in parts per million (δ) relative to tetramethylsilane (δ = 0.0) as an internal standard and coupling constants (*J*) in Hertz. Low-resolution mass spectra (ESI-MS) were recorded on LC/MS-2020 Agilent.

Synthesis of tert-Butyl 4-(2-(3,4-dimethoxyphenyl)-imidazo-[1,2-a]-pyridin-6-yl)-5,6-dihydropyridine-1(2H)-carboxylate **(15)**

To a stirred solution of 6-bromo-2-(3,4-dimethoxyphenyl)-imidazo-[1,2-a]-pyridine (**14**) (14.0g, 0.042mol) and *tert*-butyl 4-(4,4,5,5-tetramethyl-1,3,2-dioxaborolan-2-yl)-5,6-dihydropyridine-1(2*H*)-carboxylate (15.5g, 0.050 mol) in 1,4-dioxane (210 mL) was added 2M Na_2CO_3 (52.5 mL) and purged with argon gas for 10 min. $Pd(dppf)Cl_2$ (1.84 g, 0.00252 mol), was added to the mixture and continued the purging for another 5 min. The reaction mixture was heated for 16 h at 105 °C under N_2 atmosphere. After the reaction was complete, as indicated by TLC, 1,4-dioxane was evaporated under reduced pressure. The obtained residue was diluted with 200 mL of water. The compound was extracted from aqueous layer with 2×500 mL portions of EtOAc. The organic layers were collected, dried over anhydrous Na_2SO_4 and evaporated. The resultant residue was purified by column chromatography (ethyl acetate/pet ether 60%) to obtain *tert*-butyl 4-(2-(3,4-dimethoxyphenyl)-imidazo-[1,2-a]-pyridin-6-yl)-5,6-dihydropyridine-1(*2H*)-carboxylate (**15**) as pale yellow solid, yield 11.6 g (63%). ^{1}H NMR (400 MHz, DMSO-d_6): δ 8.51 (s, 1H), 8.29 (s, 1H), 7.56 (d, *J* = 7.13 Hz, 2H), 7.49 (dd, *J* = 10.63, 2.46 Hz, 2H), 7.03

(d, *J* = 8.25 Hz, 1H), 6.29 (bs, 1 H), 4.03 (bs, 2 H), 3.88 (s, 3H), 3.79 (s, 3H), 3.58 (t, *J* = 5.42 Hz, 2H), 3.46 (t, *J* = 5.40 Hz, 2H), 1.49 (s, 9H). ESI MS (m/z): calcd. for $C_{25}H_{29}N_3O_4$, 435.22, found 436.2 $[M + H]^+$.

Synthesis of 2-(3,4-Dimethoxyphenyl)-6-(1,2,3,6-tetrahydropyridin-4-yl)-imidazo-[1,2-a]-pyridine hydrochloride **(IP-NH)**

To a stirred solution of *tert*-butyl 4-(2-(3,4-dimethoxyphenyl)-imidazo-[1,2-a]-pyridin-6-yl)-5,6-dihydropyridine-1(2*H*)-carboxylate (4) (11.0 g, 0.025 mol) in 2,2,2,trifluoroethanol (220 mL) was added trimethylsilyl chloride (16.1 mL, 0.125 mmol) at 0°C and stirred for 2 h . The reaction was monitored by TLC (80% EA-Hex) and ESI MS. After completion of reaction, as indicated the TLC, the reaction mixture was evaporated under reduced pressure to obtain crude product, washed with diethyl ether and filtered and dried in vacuo to yield the desired product (**IP-NH**) as off white solid; yield 8.20 g (87%). ^{1}H NMR (400 MHz, DMSO-d_6): δ 8.51 (s, 1H), 8.29 (s, 1H), 7.56 (d, *J* = 7.13 Hz, 2H), 7.49 (dd, *J* = 10.63, 2.46 Hz, 2H), 7.03 (d, *J* = 8.25 Hz, 1H), 6.29 (bs, 1 H), 4.03 (bs, 2 H), 3.88 (s, 3H), 3.79 (s, 3H), 3.58 (t, *J* = 5.42 Hz, 2H), 3.46 (t, *J* = 5.40 Hz, 2H). ESI MS (m/z): calcd. for $C_{25}H_{29}N_3O_4$, 335.4, found 336.2 $[M + H]^+$.

General procedure for synthesis of 1-(4-(2-(3,4-Dimethoxy phenyl)-imidazo-[1,2-a]-pyridin-6-yl)-5,6-dihydropyridin-1(*2H*)-yl) amide (**IPA 1-17**)

To a stirred suspension of 2-(3,4-dimethoxyphenyl)-6-(1,2,3,6-tetrahydropyridin-4-yl)-imidazo-[1,2-a]-pyridine. Hydrochloride **(IP-NH)** (150 mg, 0.404 mmol) in dry DCM (5.0 mL) was added Hunig's base (0.18mL, 1.01 mmol) at 0 °C under N_2 atmosphere. Later, corresponding acid chloride (0.606 mmol) was added to the above solution and resultant mixture was heated to room temperature for 2 h. The reaction progress was monitored by TLC. After completion of reaction, as indicated by TLC, the reaction mass is diluted with dichloromethane and organic layer was washed with sat. $NaHCO_3$, brine, dried over anhydrous Na_2SO_4 and evaporated under reduced pressure. The resultant residue was purified by column chromatography (silica gel 100-200 mesh, ethyl acetate /pet ether 70%) to yield compounds **IPA 1-17**.

General procedure for synthesis of 2-(3,4-Dimethoxyphenyl)-6-(1-(sulfonyl)-1,2,3,6-tetrahydropyridin-4-yl)-imidazo-[1,2-a]-pyridine (IPS 1-17)

To a stirred suspension of 2-(3,4-dimethoxyphenyl)-6-(1,2,3,6-tetrahydropyridin-4-yl)imidazo-[1,2-a]-pyridine. Hydrochloride (**IP-NH**) (150 mg, 0.404 mmol) in dry dichloromethane (5.0 mL), Hunig's base (0.18 mL, 1.01 mmol) at 0 °C under N_2 atmosphere was added. Later, corresponding sulfonyl chloride (0.606 mmol) was added to the above solution and resultant mixture was heated to room temperature for 2 h. The reaction progress was monitored by TLC; after completion of reaction, as indicated by TLC, the reaction mixture was diluted with dichloromethane and organic layers were washed with saturated $NaHCO_3$, brine, dried over anhydrous Na_2SO_4 and evaporated under reduced pressure. The resultant residue was purified by column chromatography (silica gel 100-200 mesh, ethyl acetate / pet. ether 60%) to yield compounds **IPS 1-17**.

Biology Experimental procedures:

Anti-TB activity using Alamar Blue Dye

Anti-tubercular activity:

Inoculum from Löwenstein Jensen (LJ) medium was suspended in sterile Middlebrook 7H9 broth supplemented with 0.2% glycerol and 10% OADC (oleate-albumin dextrose- catalase) enrichment and a 1:20 dilution used as the inoculum for MABA. All processing was conducted with suitable safety hoods. 200 µl of sterile deionized water was added to the wells around the outer perimeter to minimize evaporation of medium during the incubation period. 100 µl of solution of each test compound was added to the wells marked 100 µg/ml and diluted with 100 µl of the broth. Serial dilution was carried out on the plate from the same using Middlebrook 7H9 broth. The final drug concentrations tested were 100, 50, 25, 12.5, 6.25, 3.125, 1.56, 0.8 and 0.4 µg/ml.

Plates were covered and sealed with parafilm after inoculation and incubated at 37ºC for five days. After the incubation period, 25 µl of a freshly prepared mixture of Alamar Blue dye and 10% tween 80(1:1 ratio) was added to the plate and incubated for 24 hrs. A blue

color in the well was interpreted as absence of bacterial growth, and pink color was scored as growth. The MIC was defined as lowest drug concentration which prevented the colour change of alamar blue from blue to pink. Inoculum from Löwenstein Jensen (LJ) medium was suspended in sterile Middlebrook 7H9 broth supplemented with 0.2% glycerol and 10% OADC (oleate-albumin dextrose- catalase) enrichment and a 1:20 dilution used as the inoculum for MABA. All processing was conducted with suitable safety hoods. 200 µl of sterile deionized water was added to the wells around the outer perimeter to minimize evaporation of medium during the incubation period. 100 µl of solution of each test compound was added to the wells marked 100 µg/ml and diluted with 100 µl of the broth. Serial dilution was carried out on the plate from the same using Middlebrook 7H9 broth. The final drug concentrations tested were 100, 50, 25, 12.5, 6.25, 3.125, 1.6, 0.8 and 0.4 µg/ml Plates were covered and sealed with parafilm after inoculation and incubated at 37ºC for five days. After the incubation period, 25 µl of a freshly prepared mixture of Alamar Blue dye and 10% tween 80 (1:1 ratio) was added to the plate and incubated for 24 hrs. A blue color in the well was interpreted as absence of bacterial growth, and pink color was scored as growth. The MIC was defined as lowest drug concentration which prevented the colour change of alamar blue from blue to pink.

Materials and methods for computational studies

In-*silico* predicted physicochemical parameters

The physicochemical parameters of the designed compounds were *in silico* predicted using the Qikprop module of Schrodinger. The diverse parameters predicted were molecular weight (M.Wt.), total solvent accessible surface area (SASA), number of hydrogen bond donors (HBD), number of hydrogen bond acceptor (HBA), octanol/water partition coefficient (log P), aqueous solubility (Log S), predicted apparent Caco-2 cell permeability in nm/sec (PCaco) and number of rotatable bonds (Rot).

Molecular docking studies

Docking studies of the significantly active compound were performed using the Glide module of Schrodinger software, version 2019-1.[1] Installed on Intel XenonW3565 processor and Ubuntu enterprise version 14.04 as an operating system. The selected target protein structure was retrieved from the RCSB protein data bank. [2] (PDB-1P44, https://www.rcsb.org/structure/4TZK).

Ligand preparation

The ligand used as an input for docking study was sketched in ChemDraw 16.0. Then, the ligand was incorporated into the workstation, and the energy was minimized using the OPLS3e (Optimized Potentials for Liquid Simulations) force field in the Ligprep module (Version 2019-1, Schrodinger) of the software.[3] This minimization helps to allocate bond orders, the addition of hydrogens to the ligands, and conversion of 2D to 3D structure for the docking studies. The generated output file (Best conformations of the ligands) was further used for docking studies.[4]

Protein preparation

Protein preparation wizard (Version 2019-1, Schrodinger).[5] Is the primary tool in Schrodinger to prepare and minimize the energy of protein. Hydrogen atoms were added to the protein, and charges were assigned. The Het states were generated using Epik at pH 7.0 ± 2.0. The protein was pre-processed, refined, modified by analyzing the workspace water molecules and other atoms. The critical water molecules remained the same, and the rest of the molecules apart from heteroatoms from the water was deleted. Finally, the protein was minimized using the OPLS3 force field. A grid was created by considering the co-crystal ligand, which was included in the active site of the selected protein target (PDB-4TZK). After the final step of docking with the co-crystal ligand in XP mode, root mean square deviation (RMSD) was checked to validate the protein. [5]

Receptor grid generation

A receptor grid was generated around the protein (PDB-4TZK) by choosing the inhibitory ligand (X-ray pose of the ligand in the protein). The centroid of the ligand was selected to create a grid box around it, and the Van der Waal radius of receptor atoms was scaled to 1.00 Å with a partial atomic charge of 0.25.

Molecular dynamics studies

Molecular Dynamics (MD) simulation helps envisage the Protein-Ligand complex's (PLC) actions at the target's binding site region in the physiological conditions. MD was performed using the Desmond module of Schrödinger developed by D.E Shaw research group (Academic license, Version 2020-1).[6] Through the system's builder panel; the orthorhombic simulation box was prepared with the

Simple Point-Charge (SPC) explicit water model in such a way that the minimum distance between the protein surface and the solvent surface is 10 Å. Protein-ligand docked complexes were solvated using the orthorhombic SPC water model.[7] The solvated system was neutralized with counter ions, and physiological salt concentration was limited to 0.15 M. The receptor-ligand complex system was designated with the OPLS AA force field.[8]

The Reversible reference System Propagator Algorithms (RESPA) integrator.[9] Nose-Hoover chain thermostat [10] , and Martyna-Tobias-Klein barostat were used with two ps relaxation times. The equilibrated system was used for the final production of the MD simulation. The production of MD simulation was run for 100 ns at 300 K temperatures at 1.0 bar pressure with NPT (Isothermal-Isobaric ensemble, constant temperature, constant pressure, constant number of particles) ensemble.[11] with the default settings of relaxation before simulation.

The MD simulation was run by using the MD simulation tool, simulation time setup to 100 ns. Further, for viewing the trajectories and creating a movie, _out file used. CMS file was imported, and the movie was exported with high resolution (1280 × 1024) with improved quality. During the MD simulation, the trajectory was written with 1000 frames. To understand the stability of the complex during MD simulation, the protein backbone frames were aligned to the backbone of the initial frame. Finally, the analysis of the simulation interaction diagram was achieved after loading the outacts file and selected Root Mean Square Deviation (RMSD) and Root Mean Square Fluctuation (RMSF) in the analysis type to obtain the mentioned plots.[12,13]

[1]H NMR spectral data for IPA and IPS series compounds

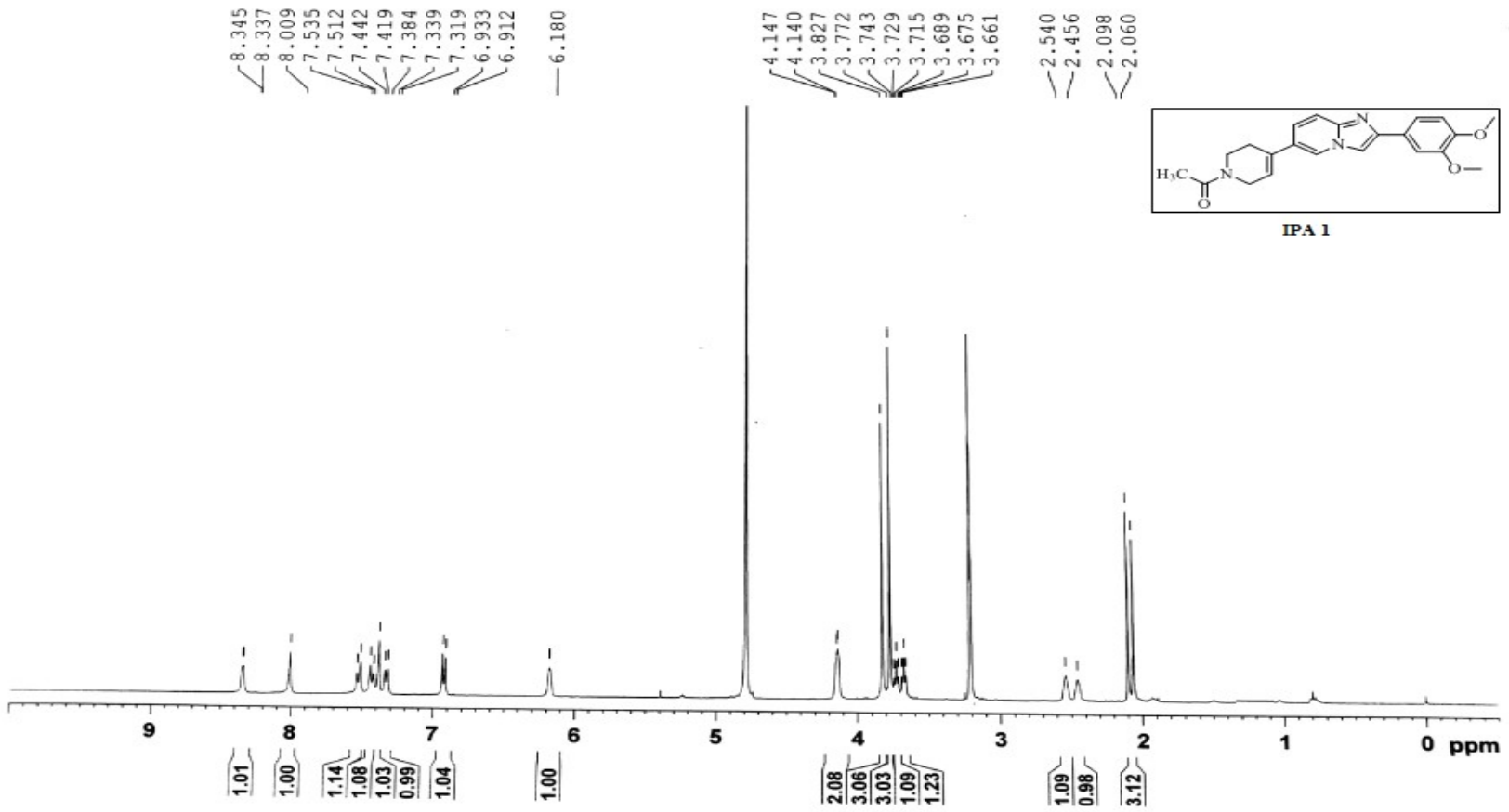

[1]H NMR spectrum of compound **IPA-1**

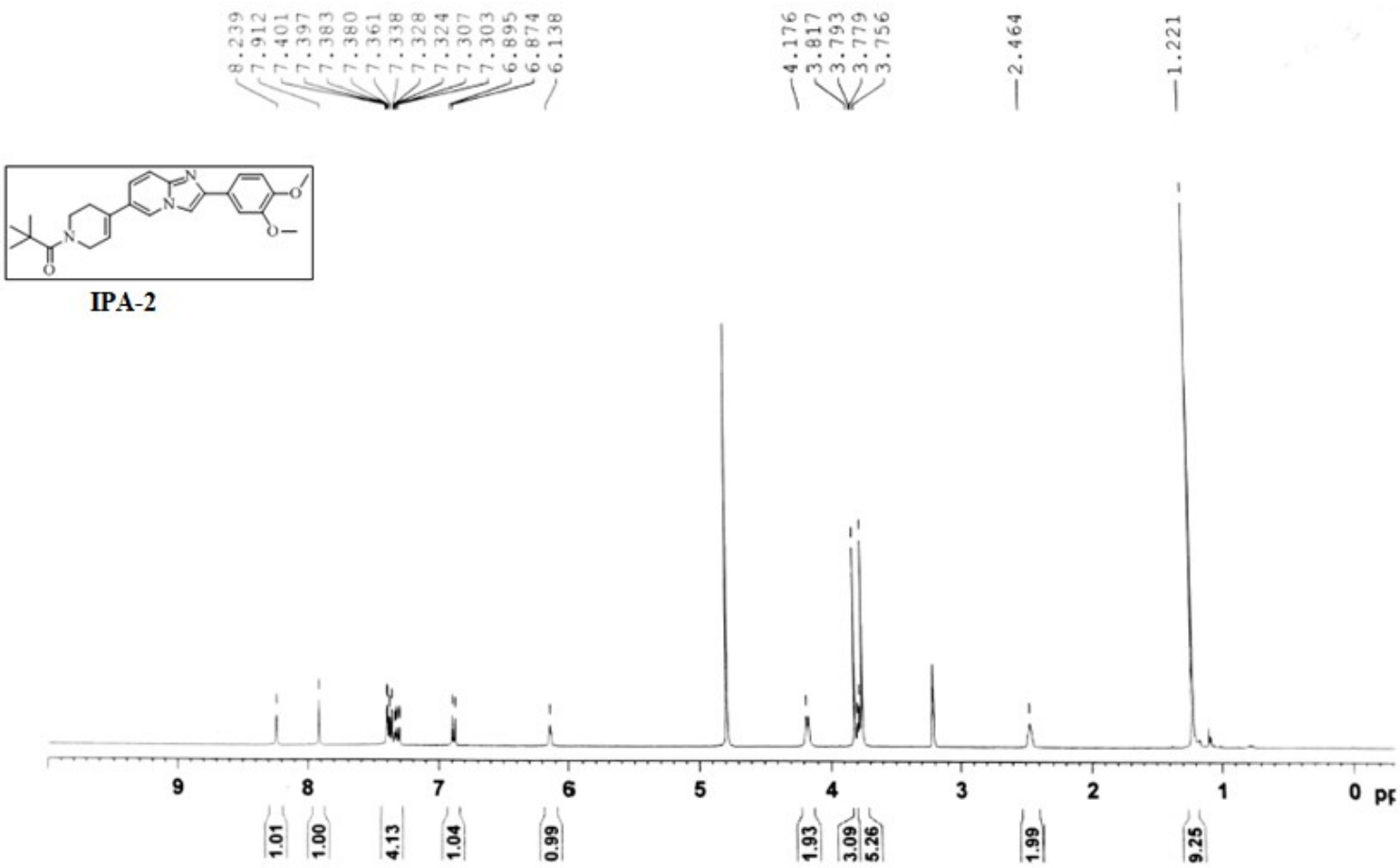

^{1}H NMR spectrum of compound **IPA-2**

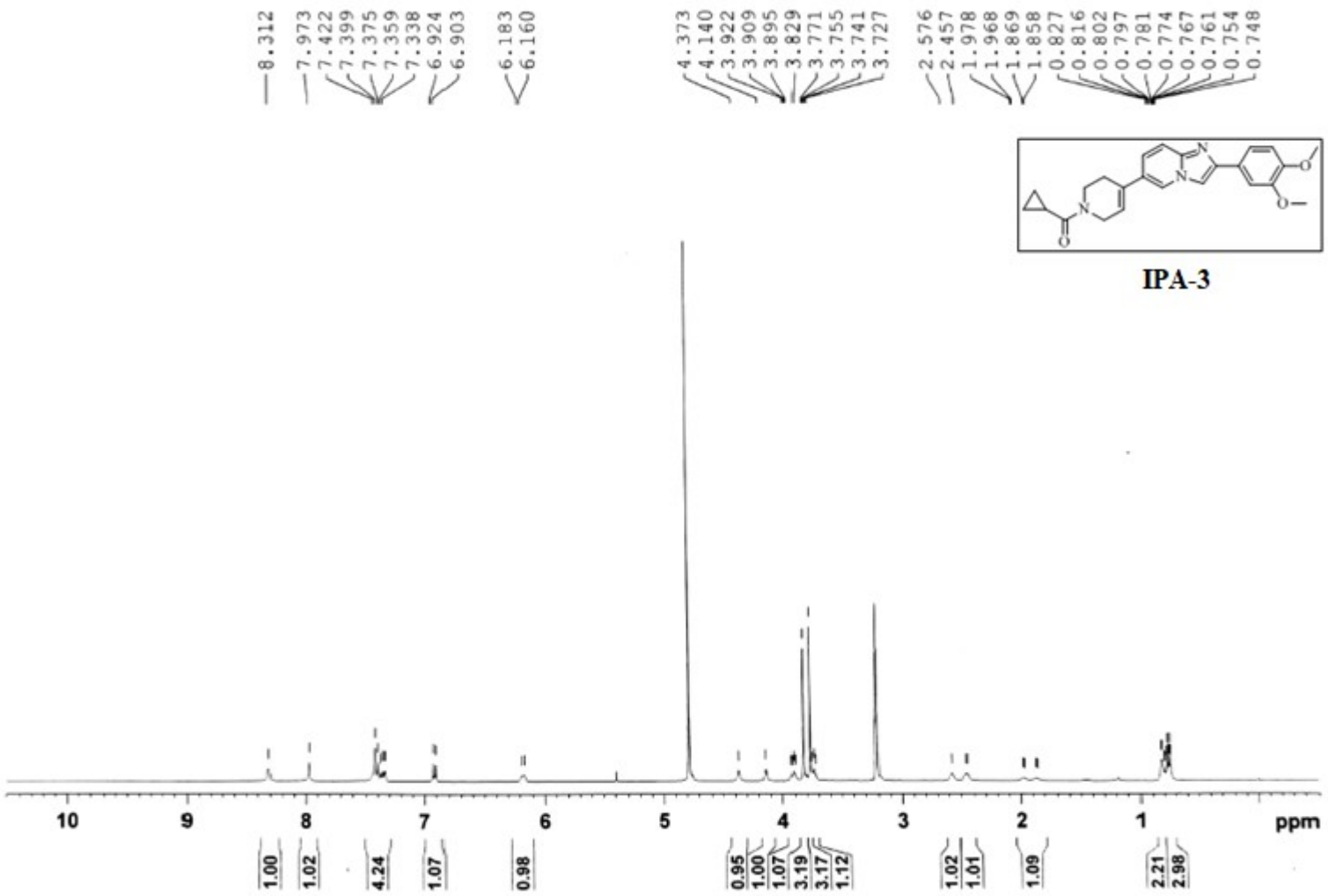

^{1}H NMR spectrum of compound **IPA-3**

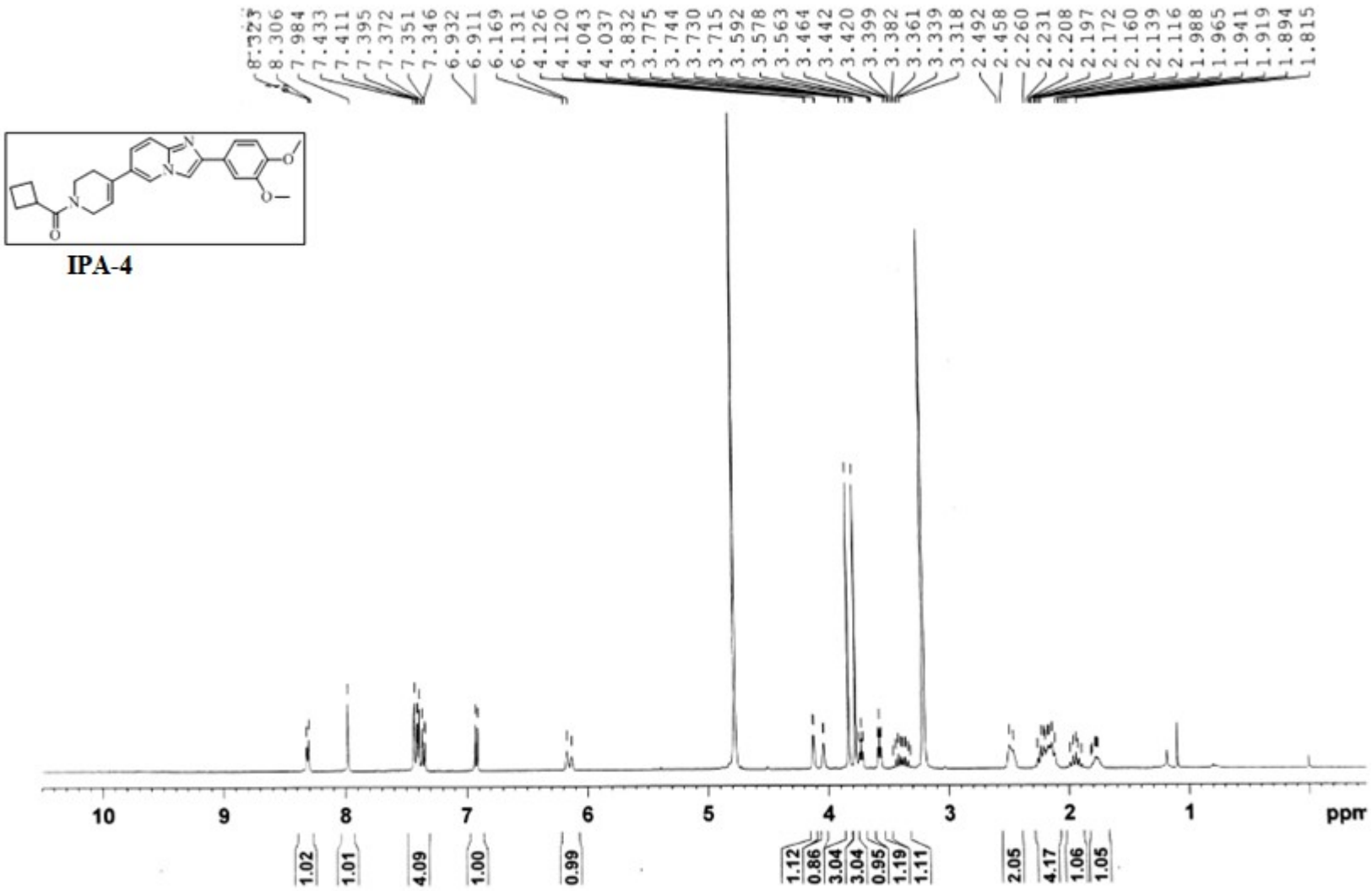

^{1}H NMR spectrum of compound **IPA- 4**

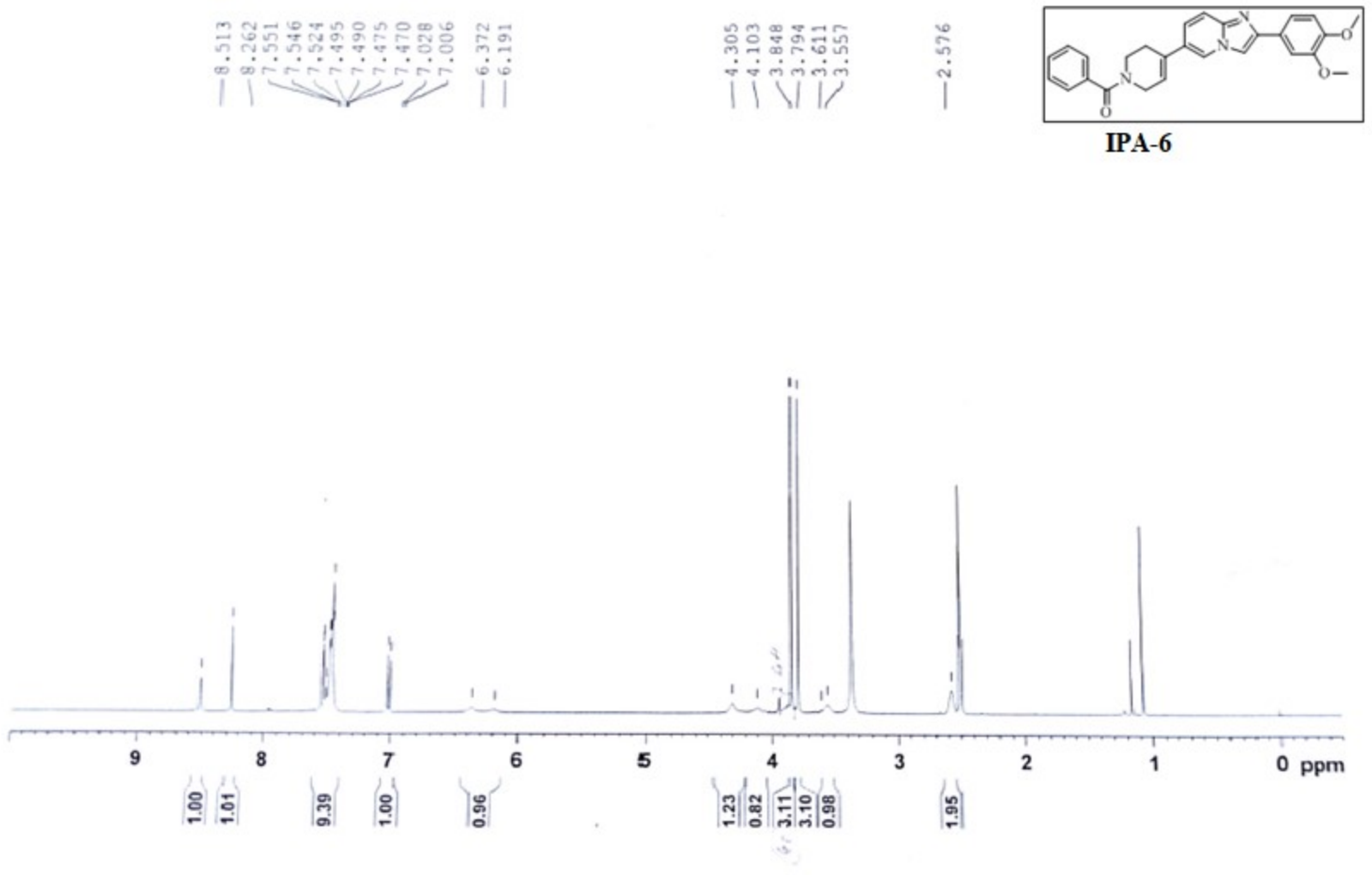

^{1}H NMR spectrum of compound **IPA-6**

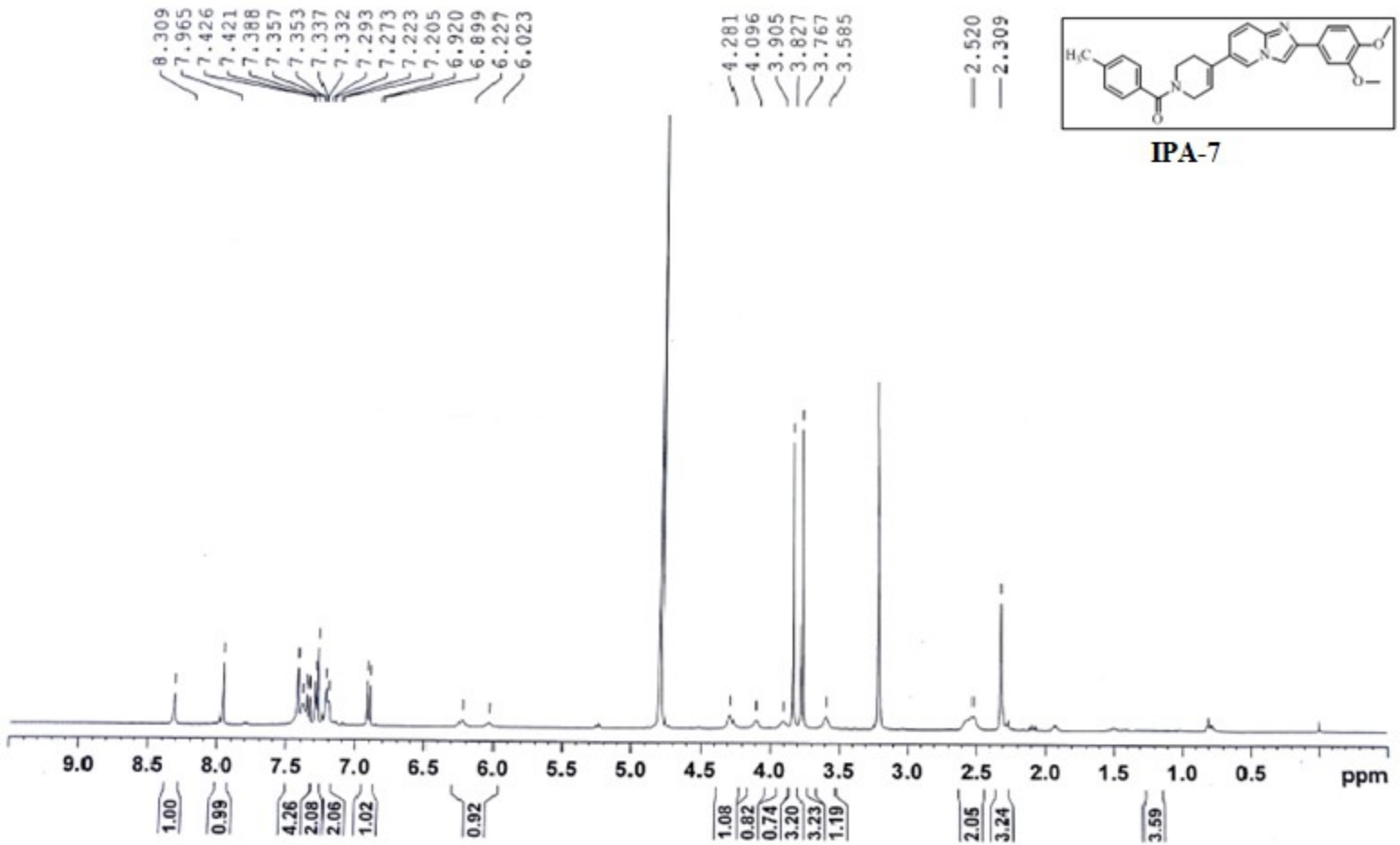

^{1}H NMR spectrum of compound **IPA-7**

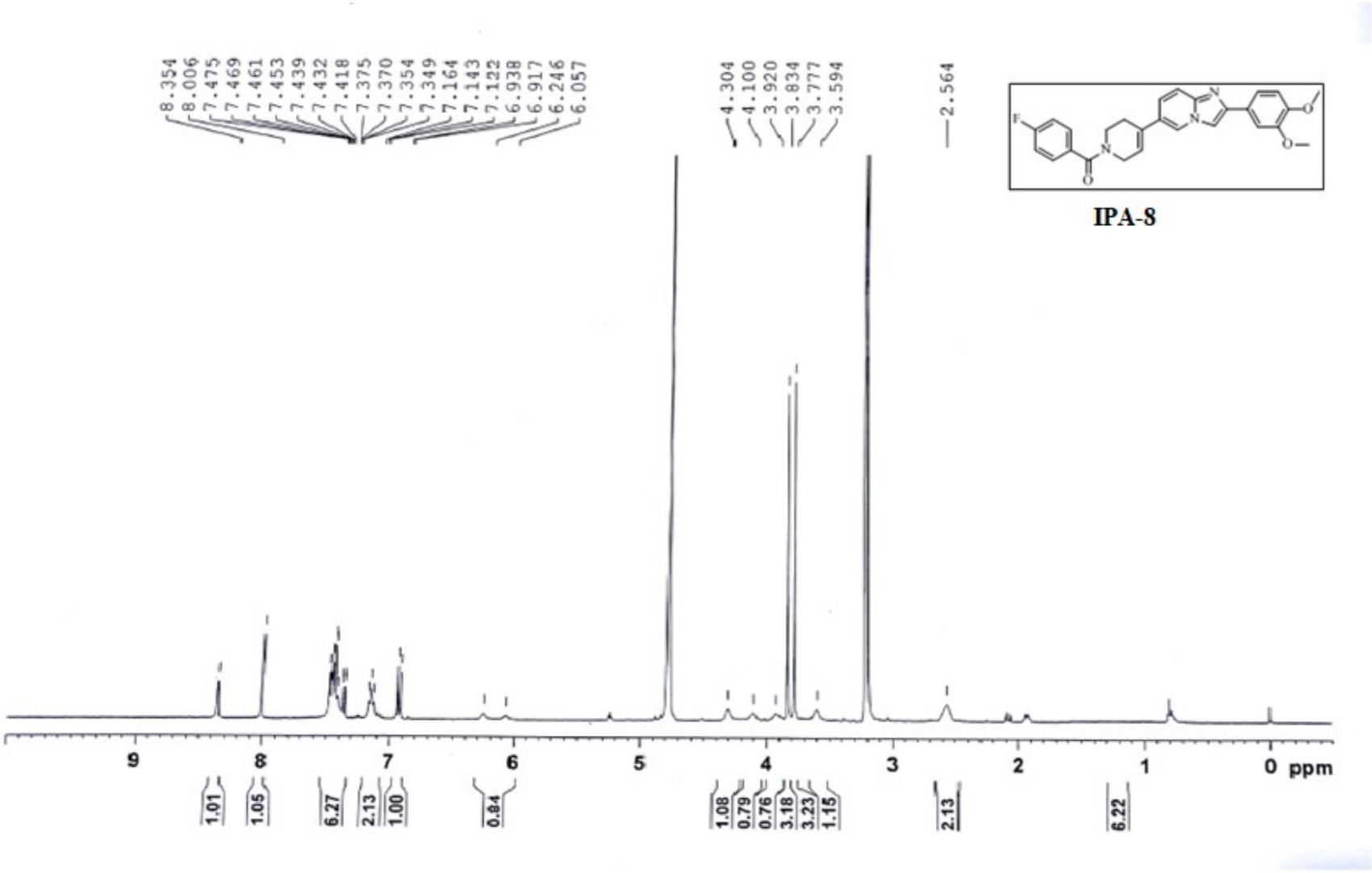

^{1}H NMR spectrum of compound **IPA-8**

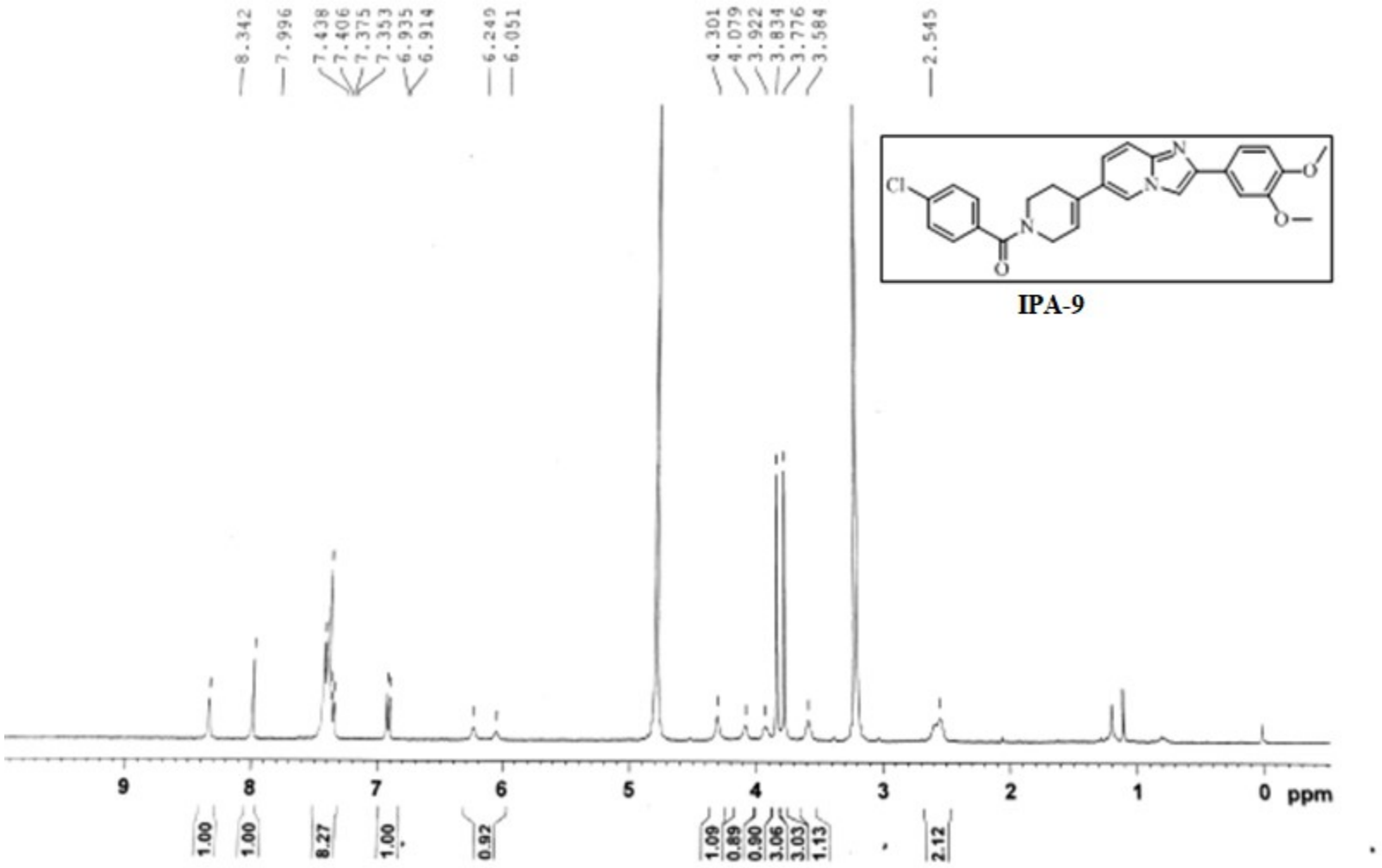

^{1}H NMR spectrum of compound **IPA-9**

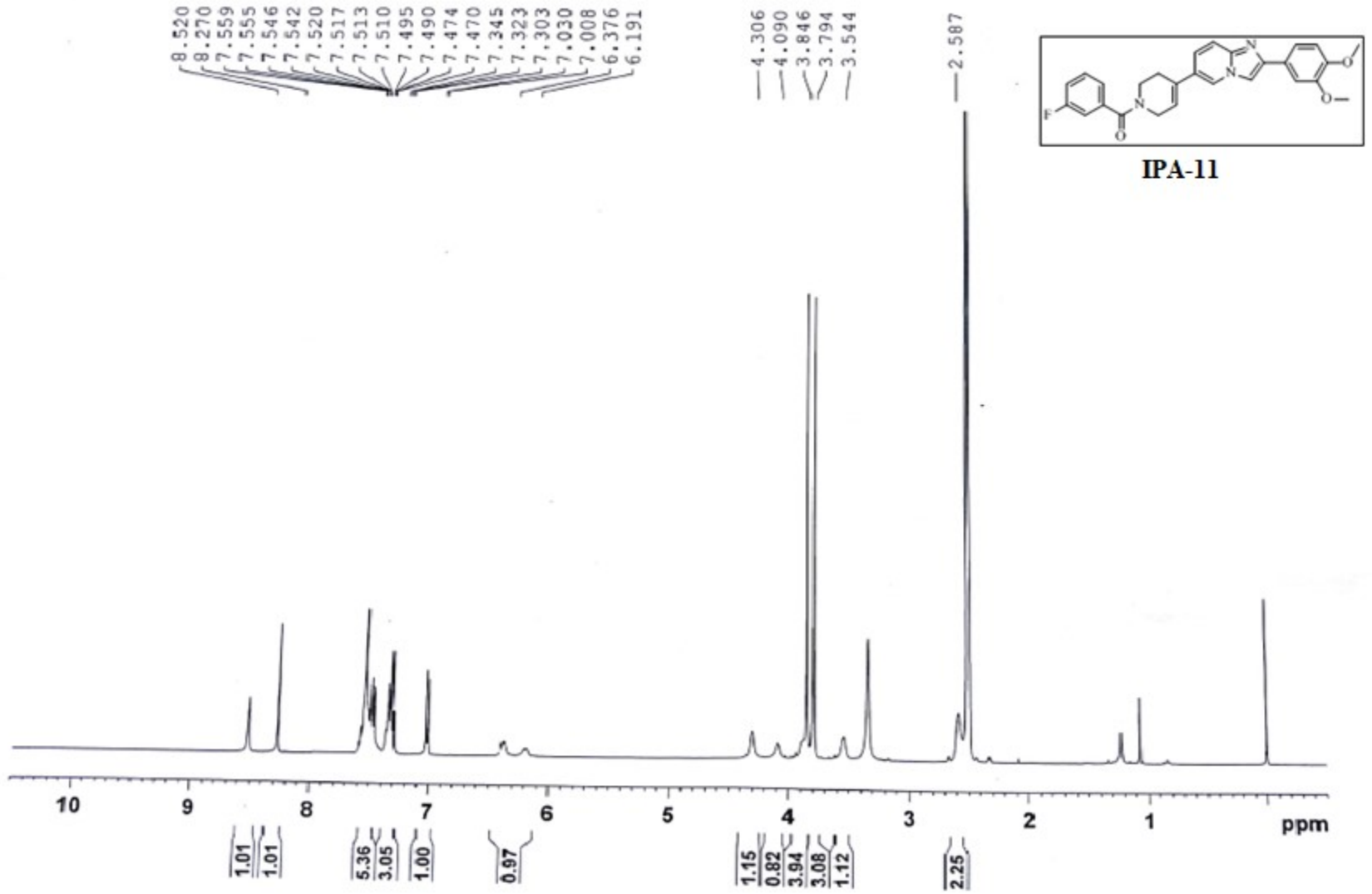

^{1}H NMR spectrum of compound **IPA-11**

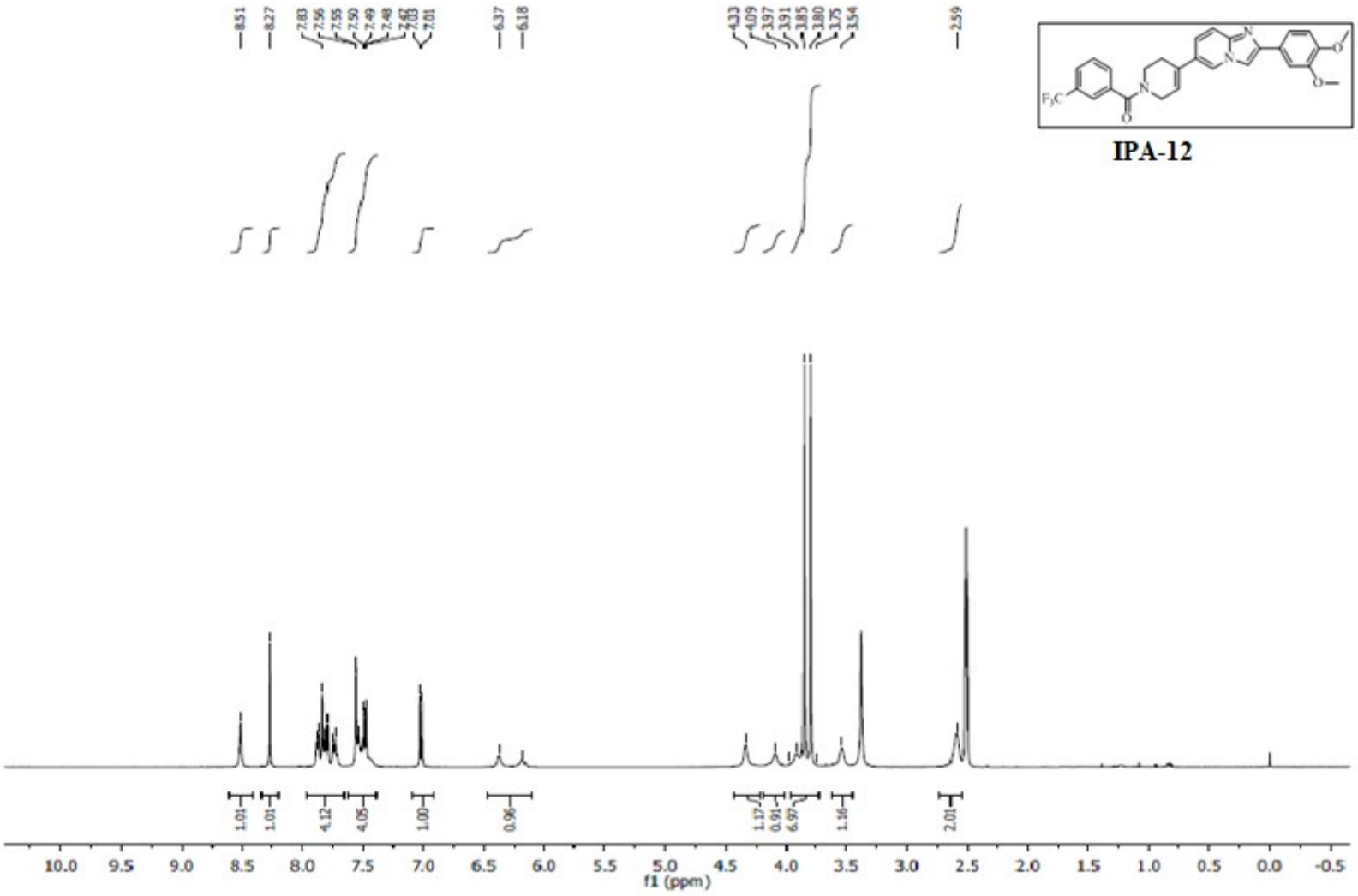

IPA-12

^{1}H NMR spectrum of compound **IPA-12**

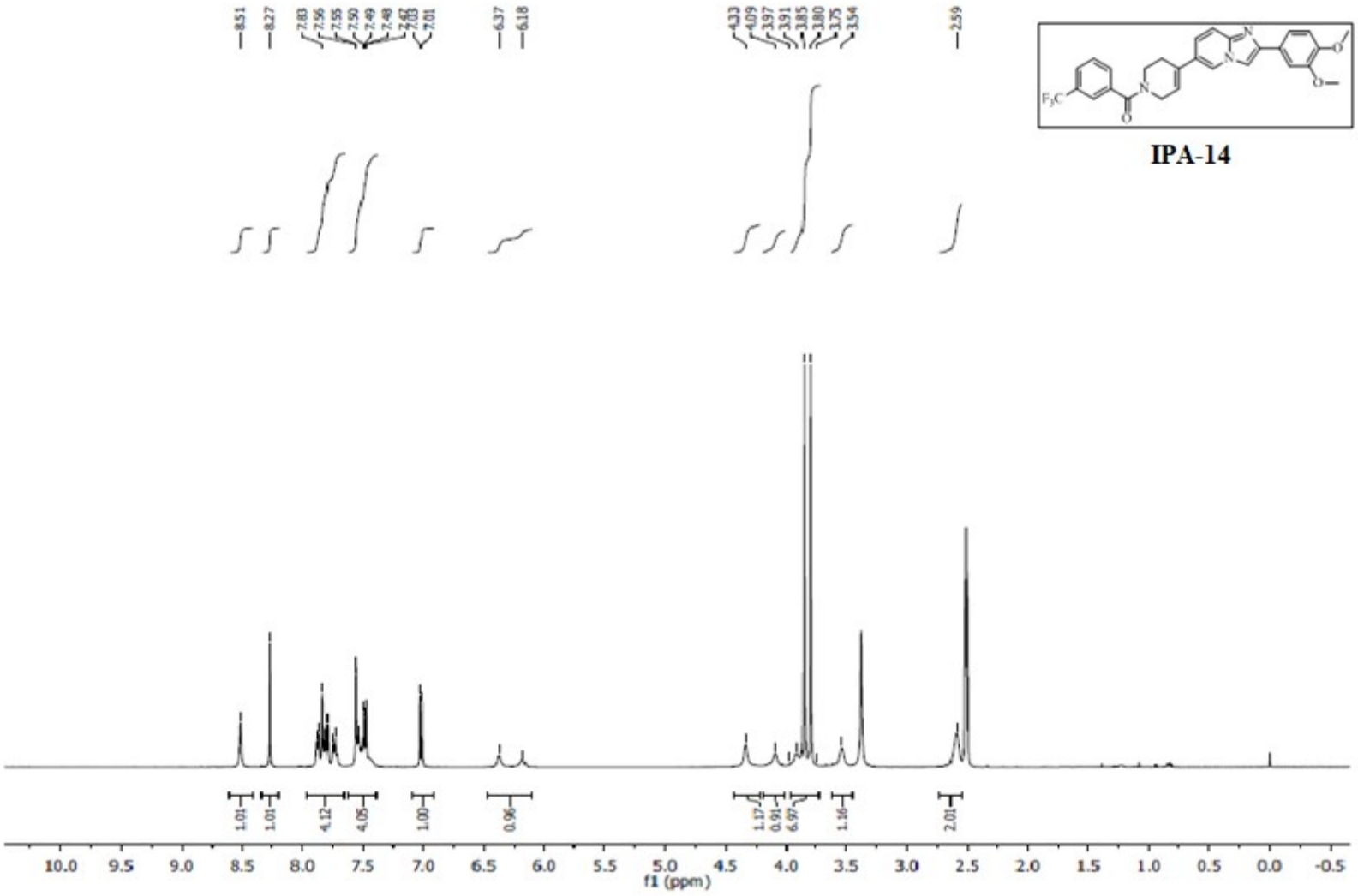

^{1}H NMR spectrum of compound **IPA-14**

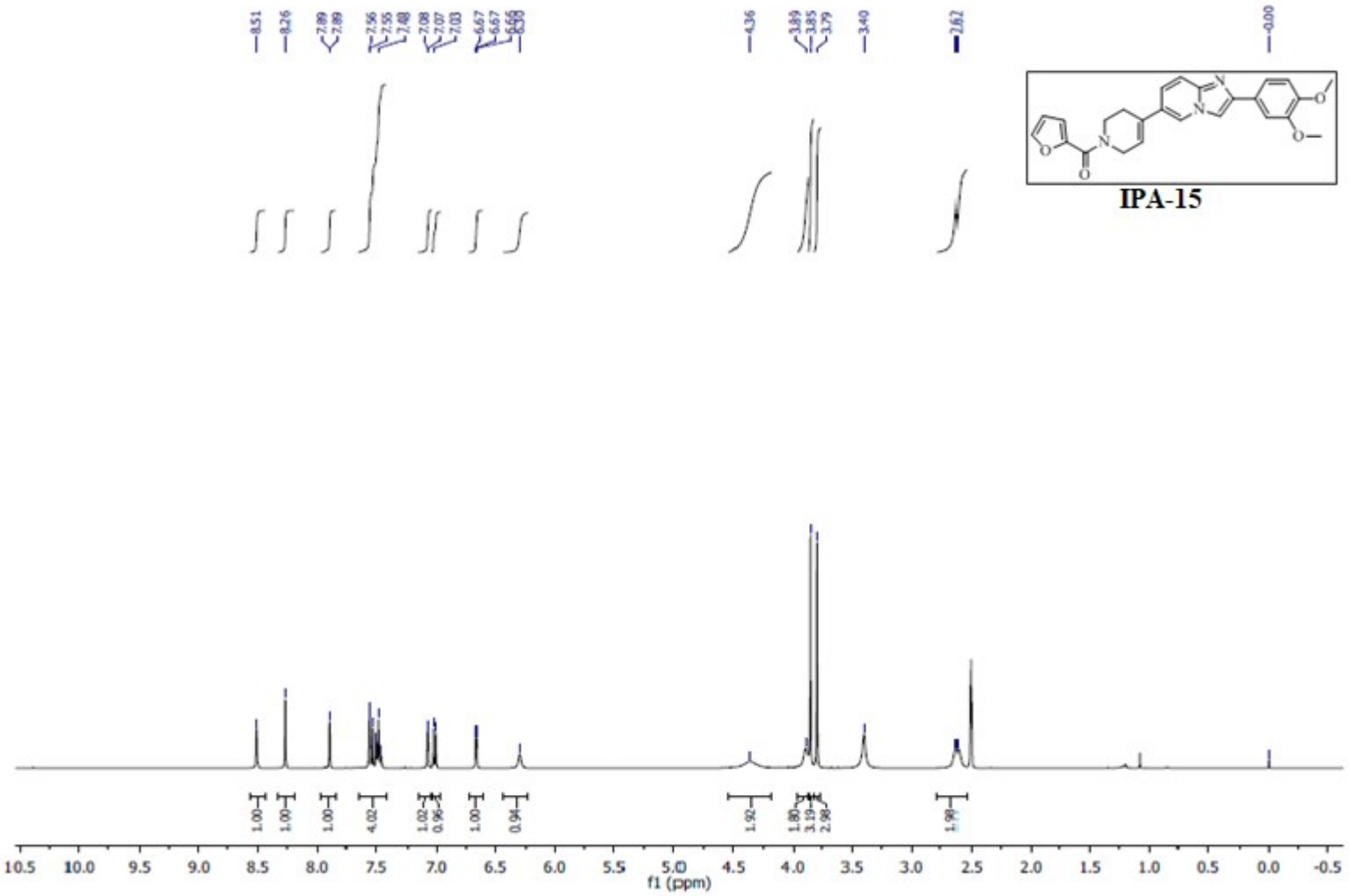

^{1}H NMR spectrum of compound **IPA-15**

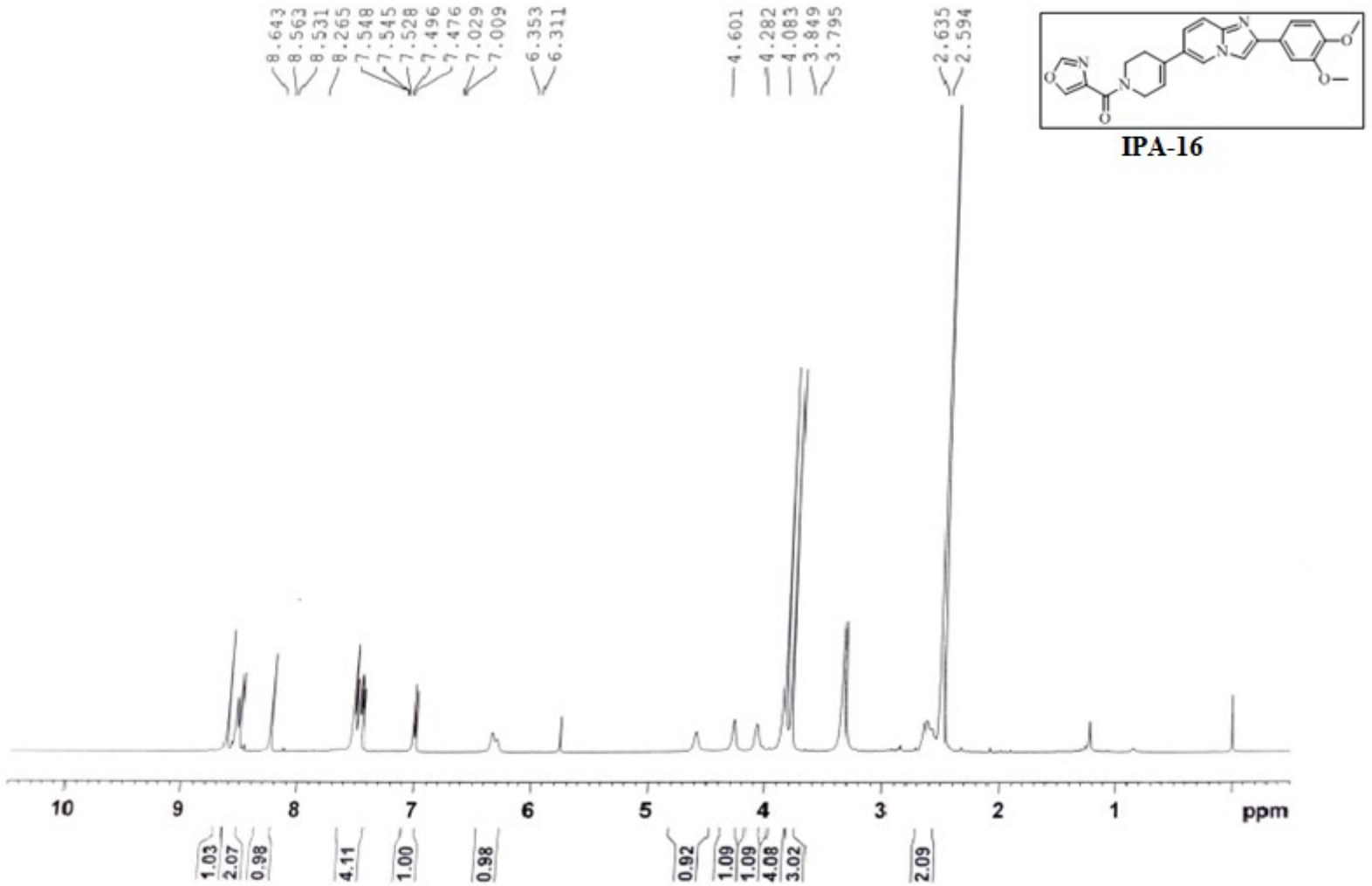

^{1}H NMR spectrum of compound **IPA-16**

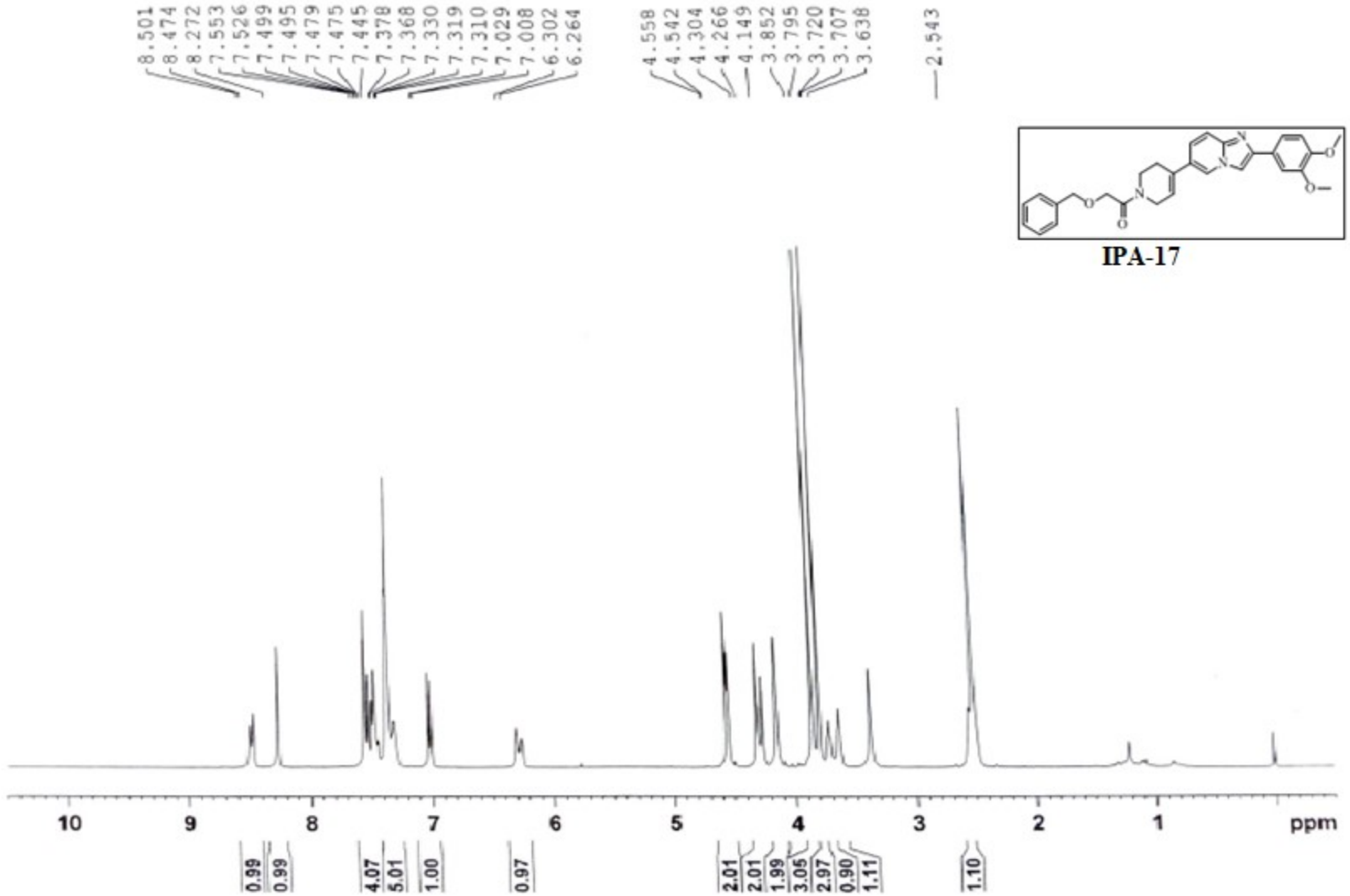

^{1}H NMR spectrum of compound **IPA-17**

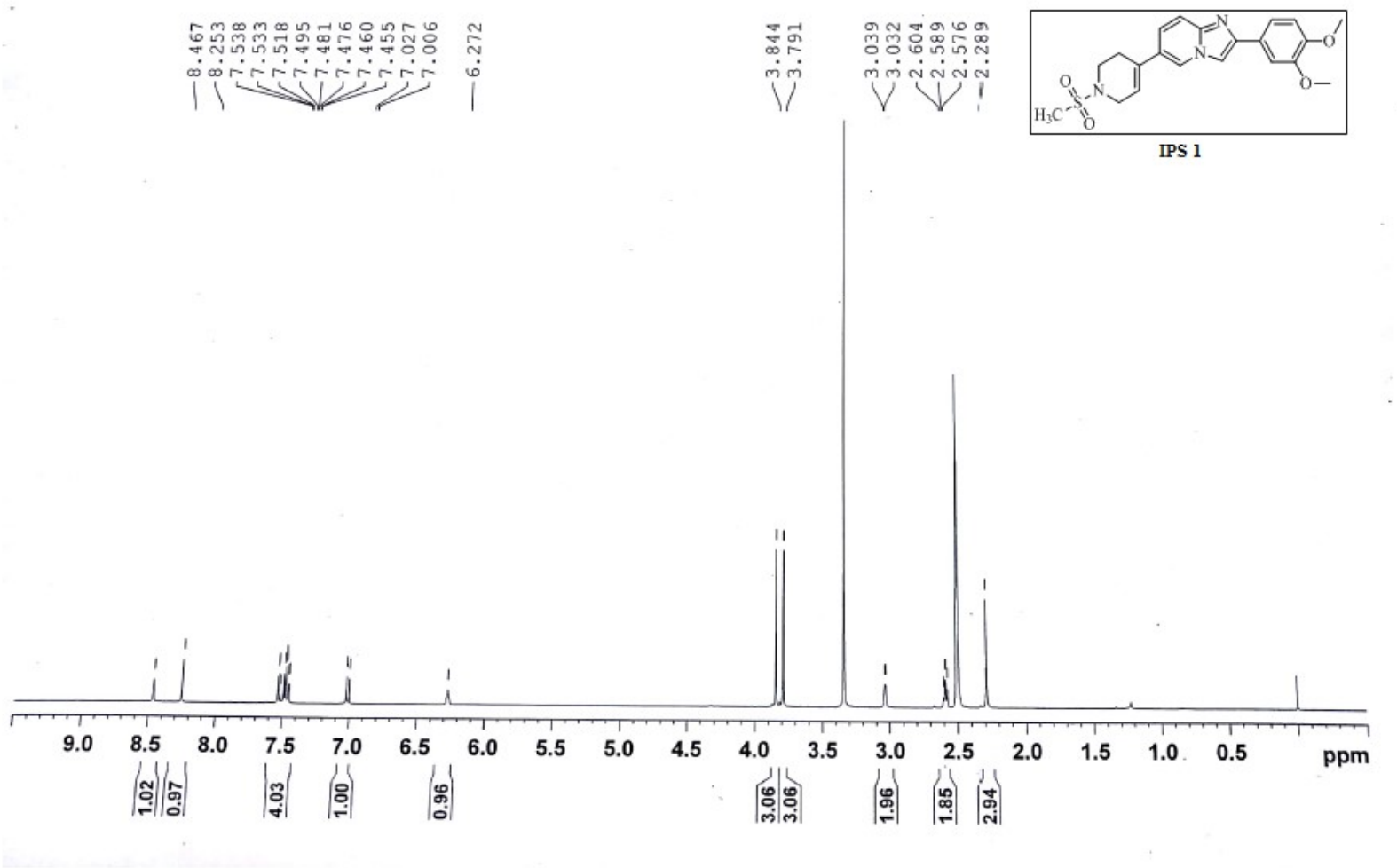

^{1}H NMR spectrum of compound **IPS-1**

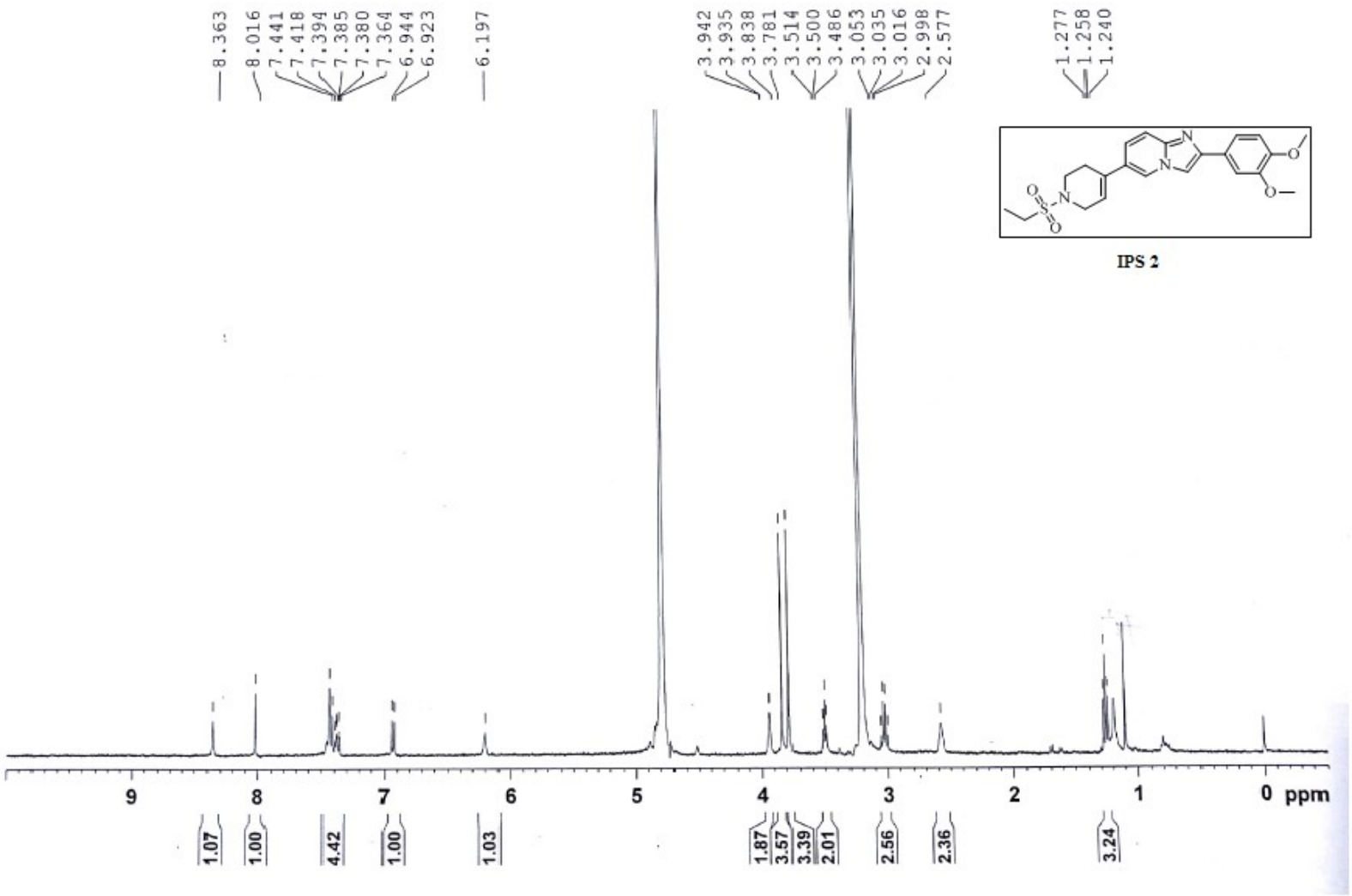

^{1}H NMR spectrum of compound **IP -2**

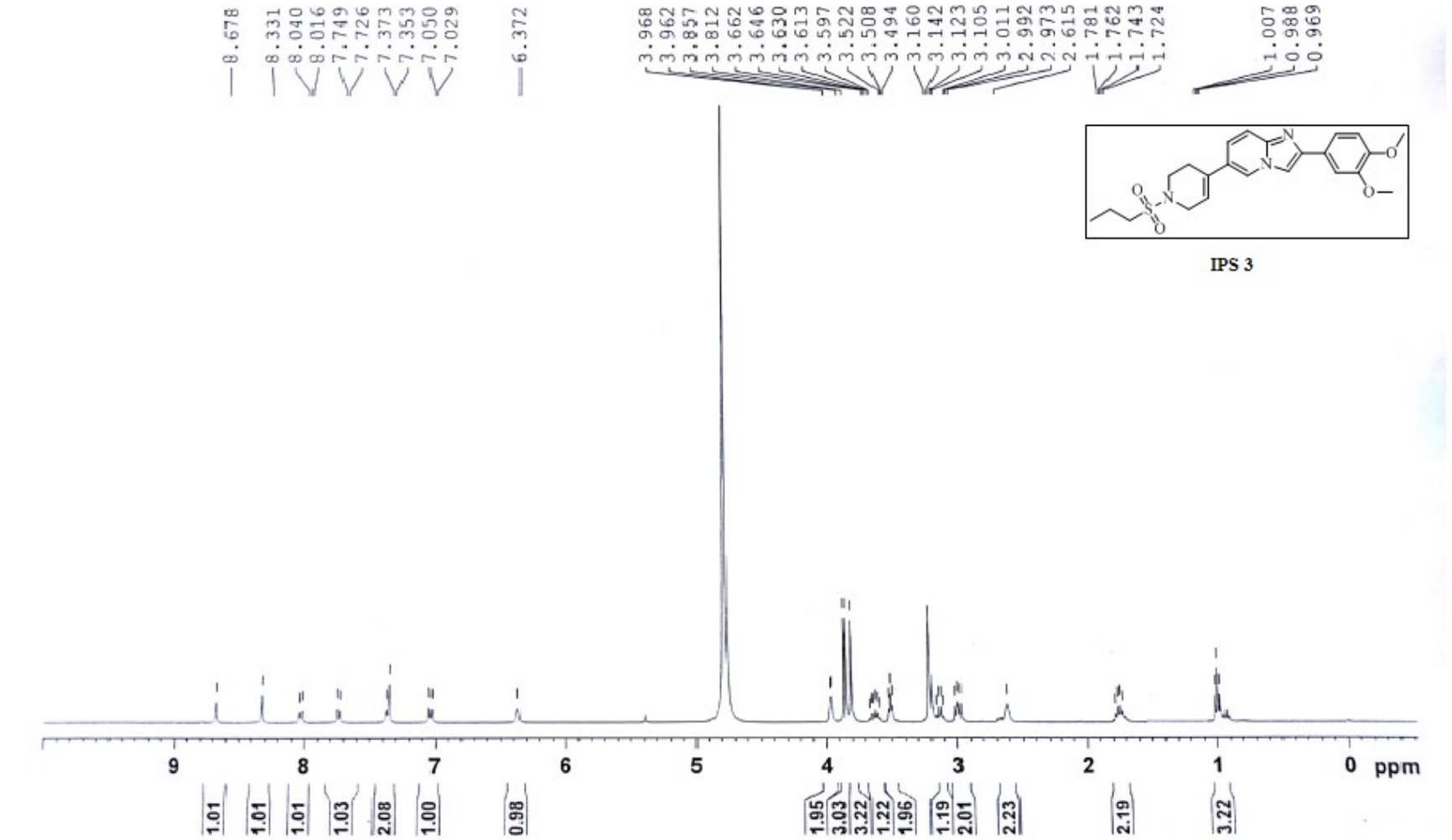

^{1}H NMR spectrum of compound **IPS-3**

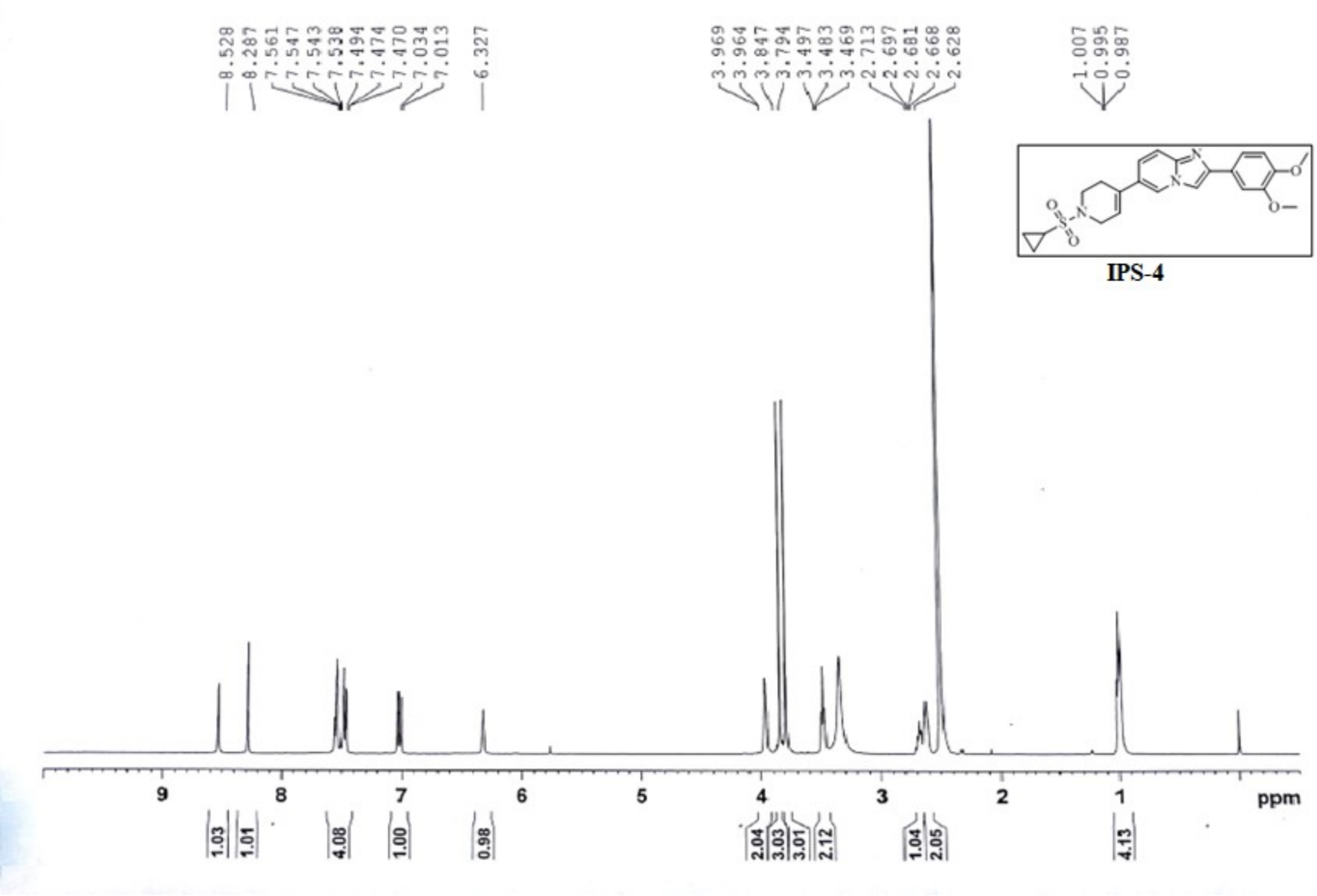

^{1}H NMR spectrum of compound **IPS-4**

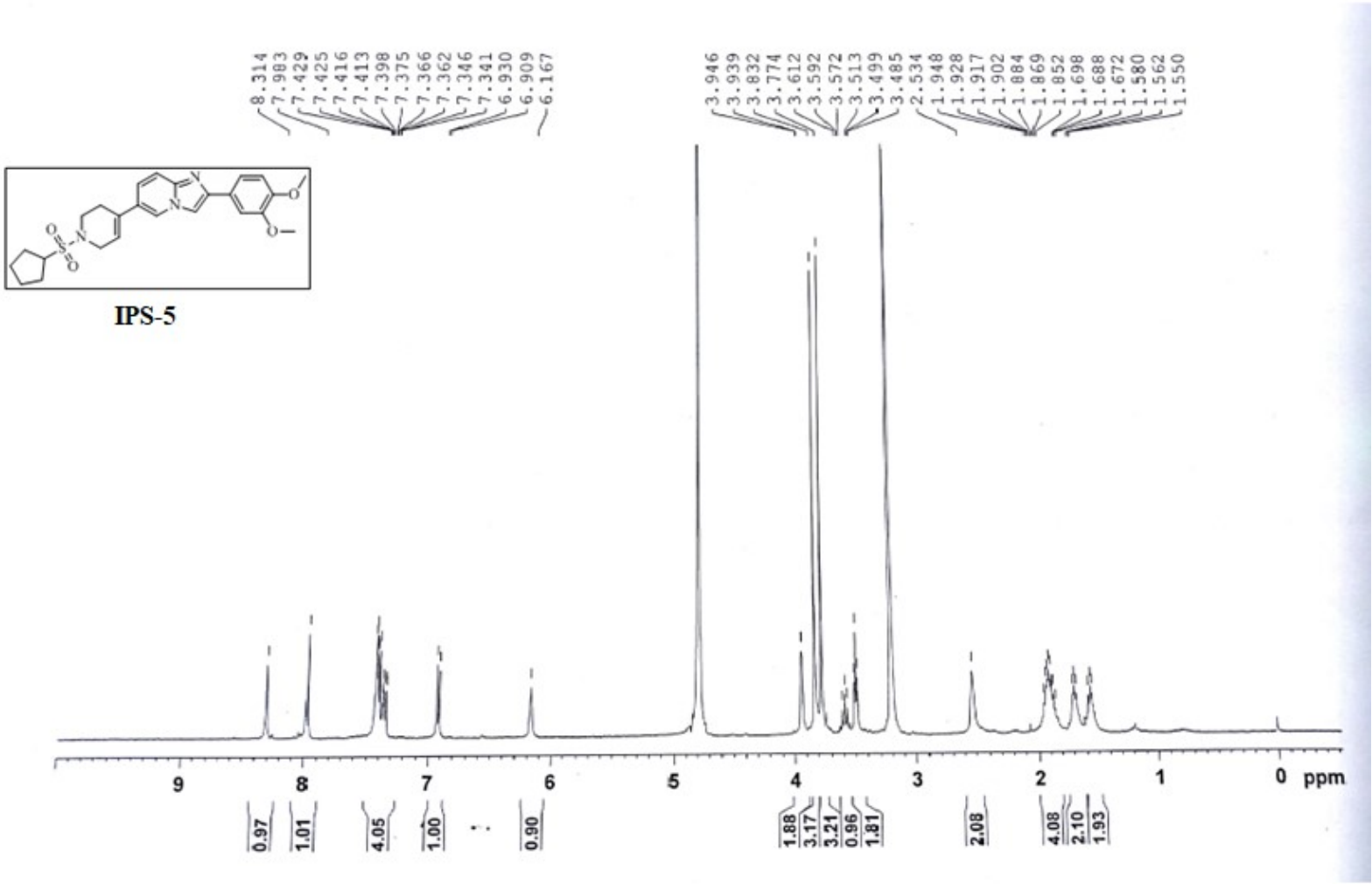

^{1}H NMR spectrum of compound **IPS-5**

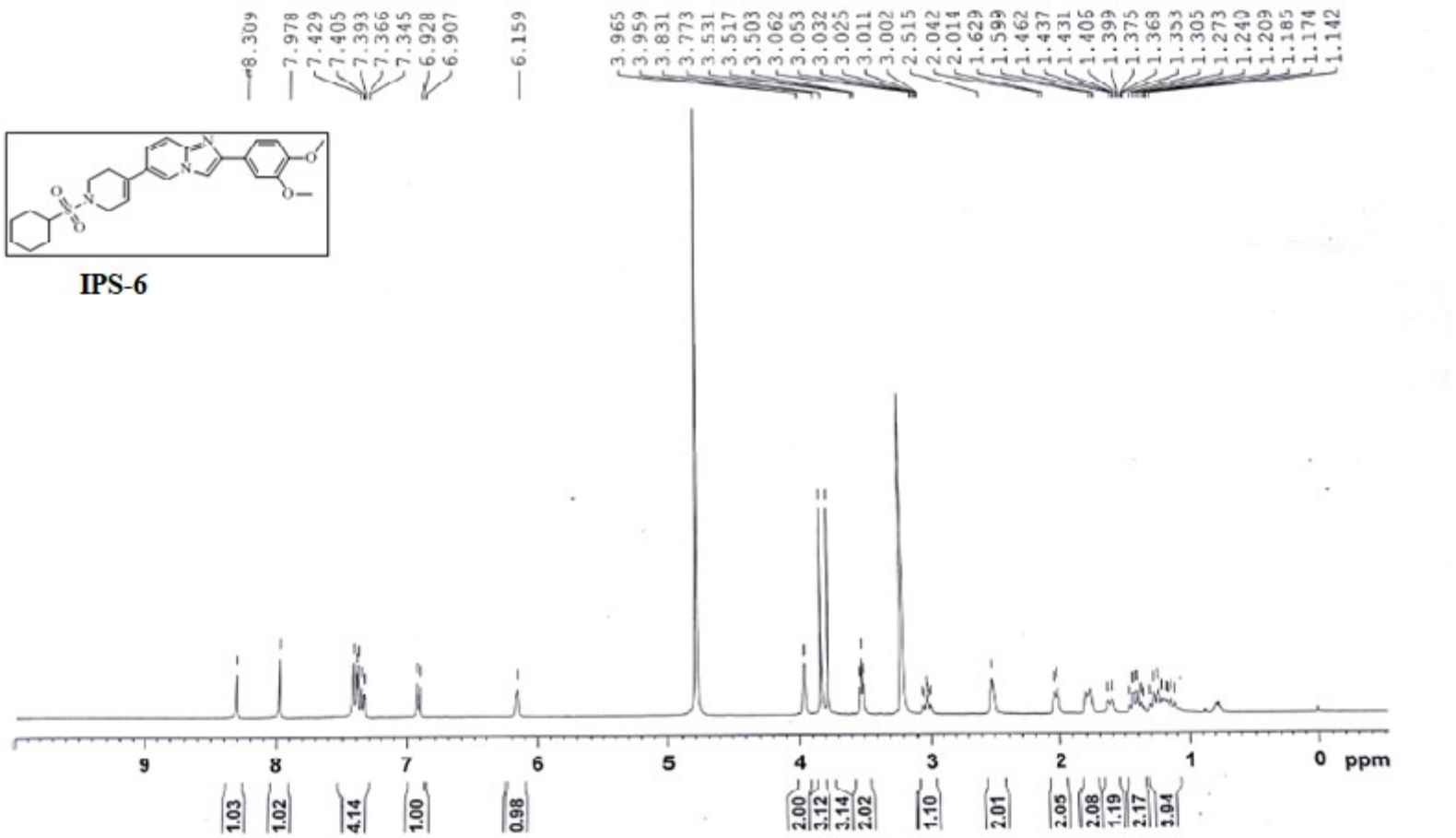

^{1}H NMR spectrum of compound **IPS-6**

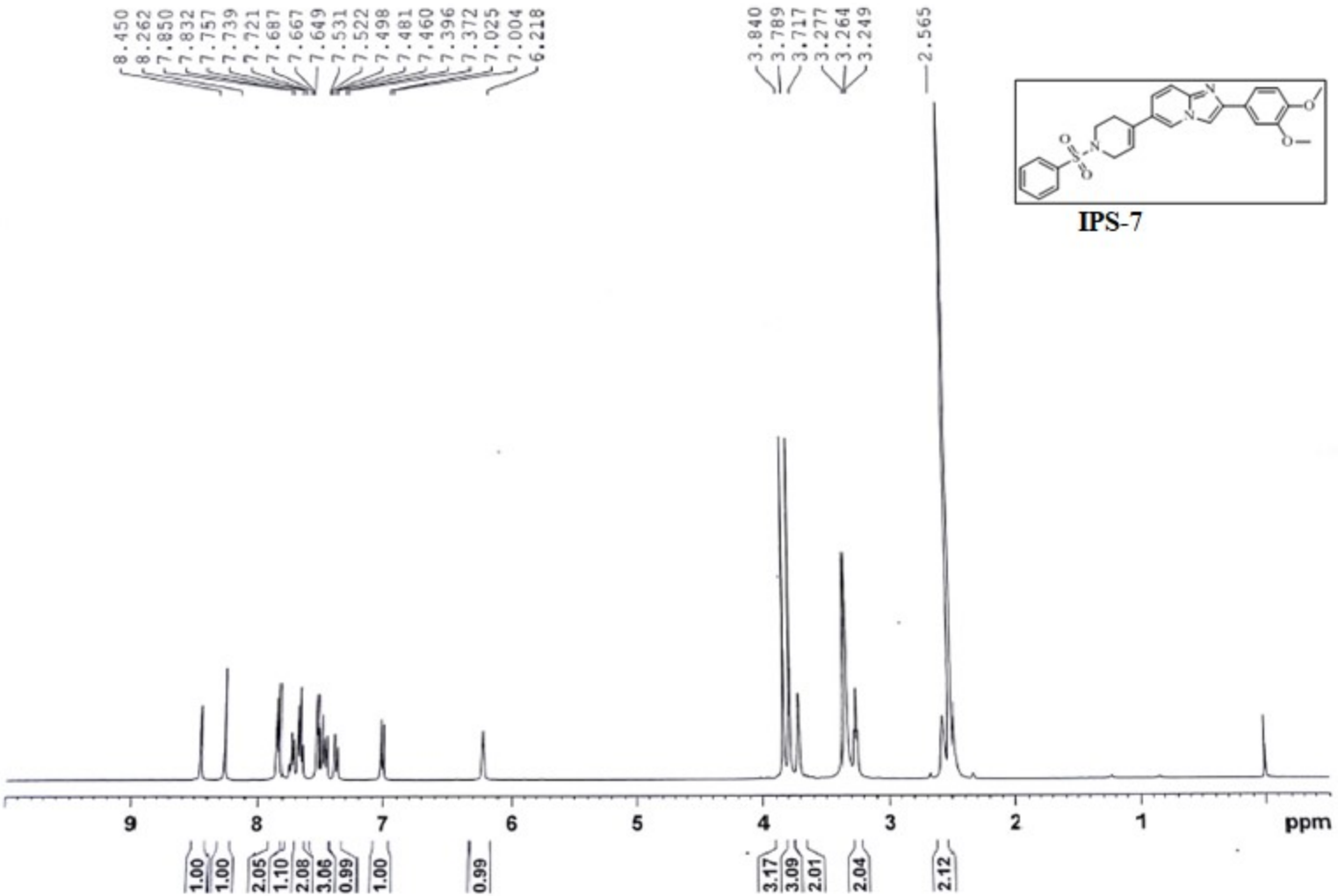

^{1}H NMR spectrum of compound **IPS-7**

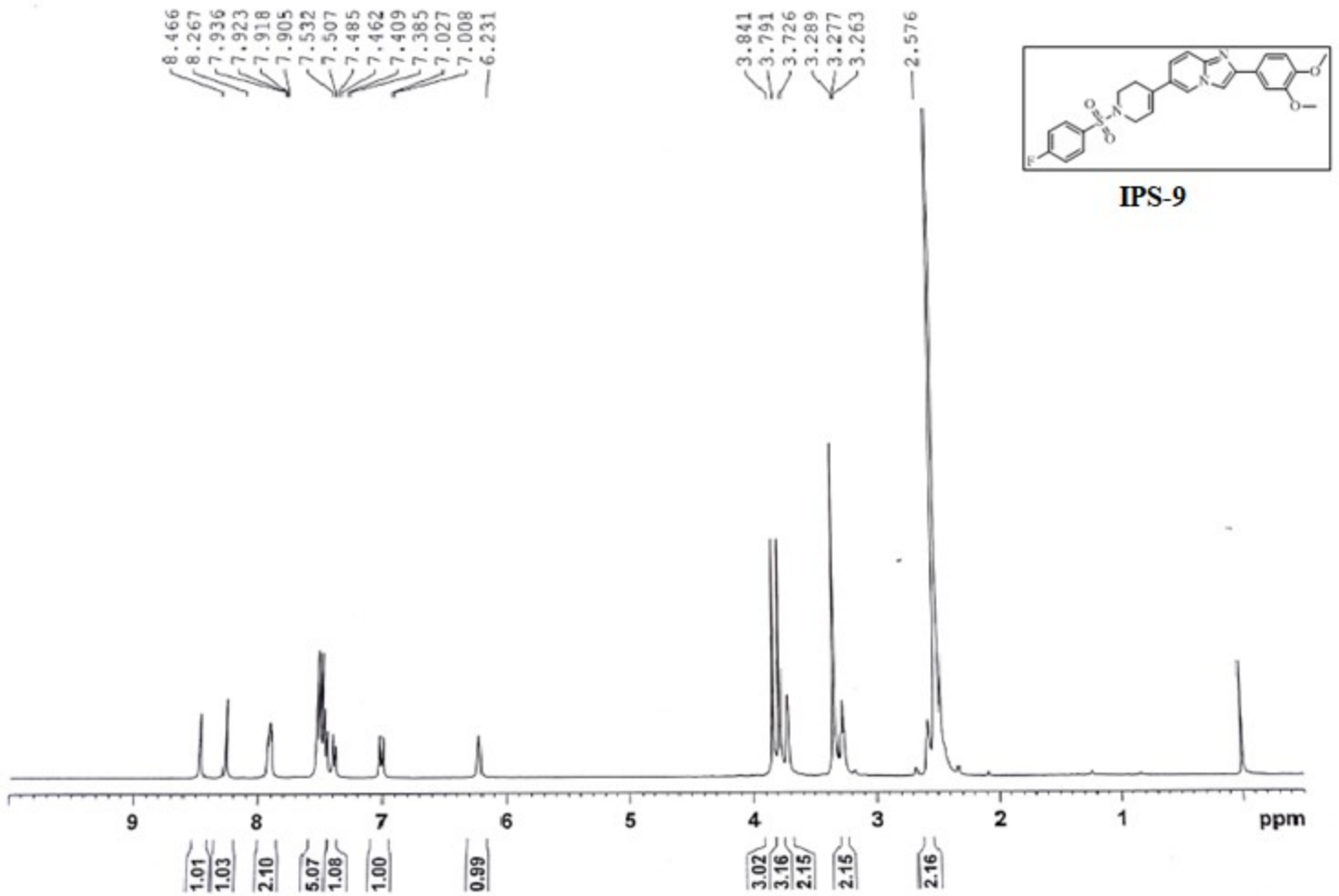

^{1}H NMR spectrum of compound **IPS-9**

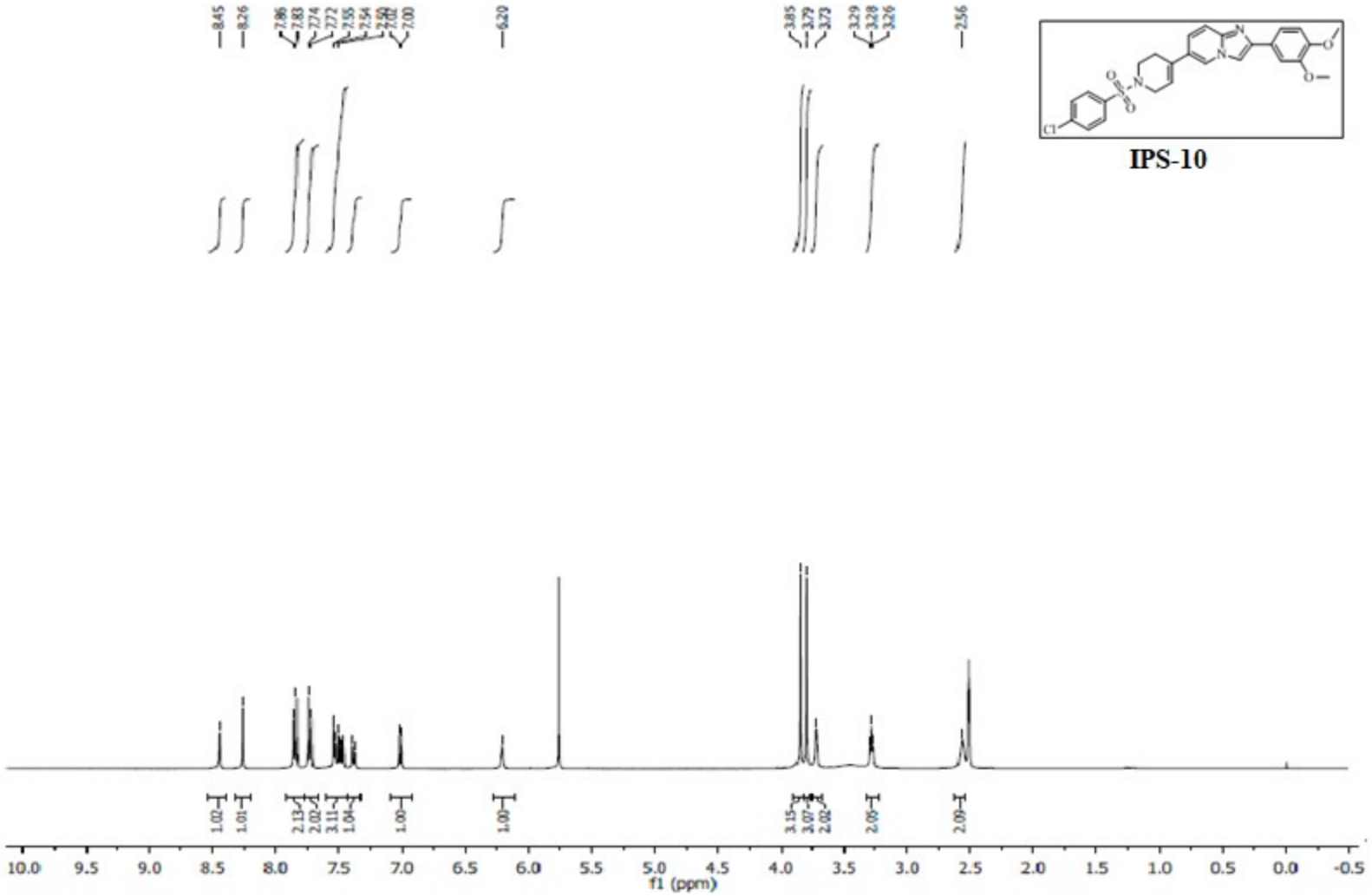

^{1}H NMR spectrum of compound **IPS-10**

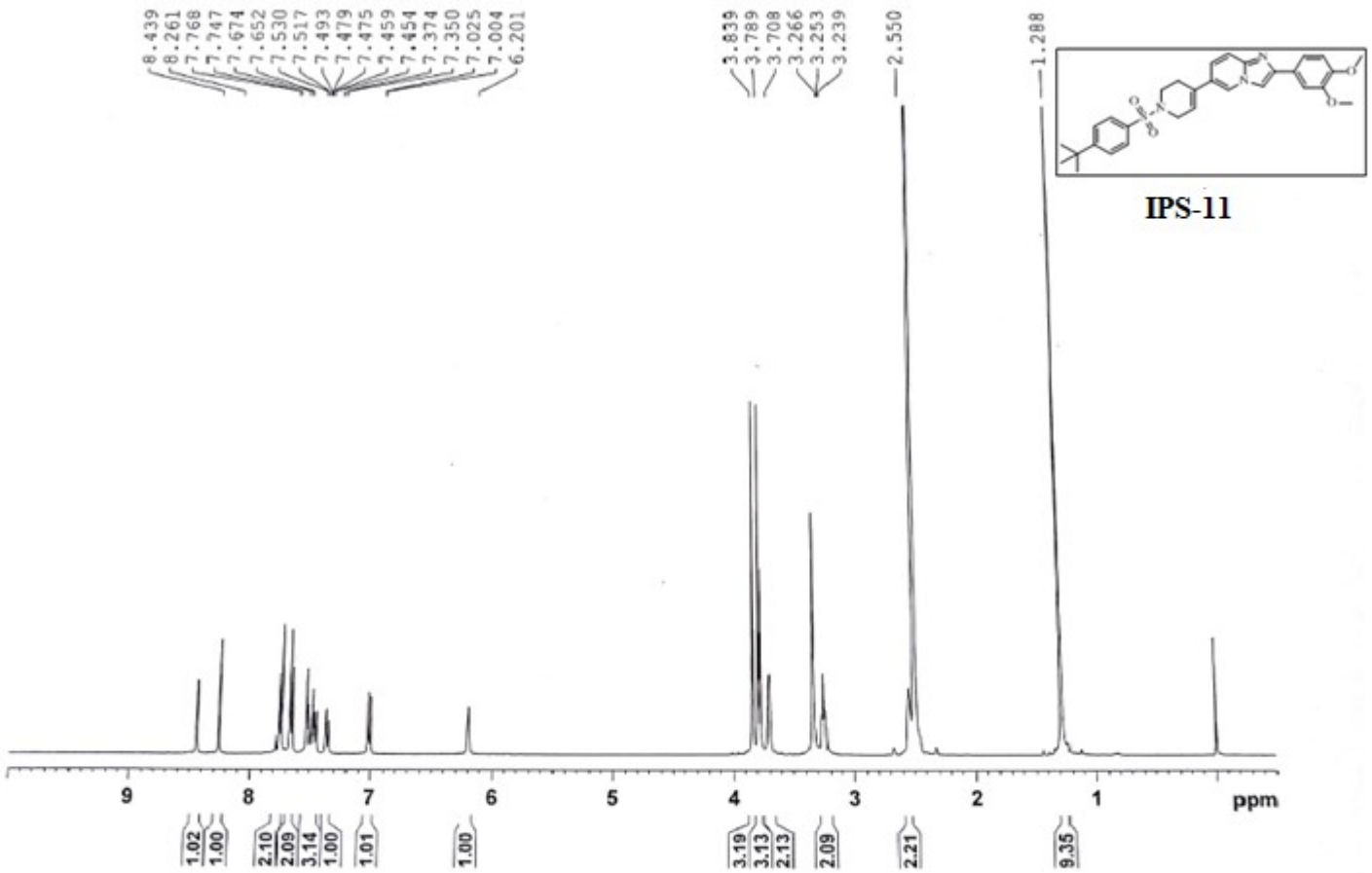

[1]H NMR spectrum of compound **IPS-11**

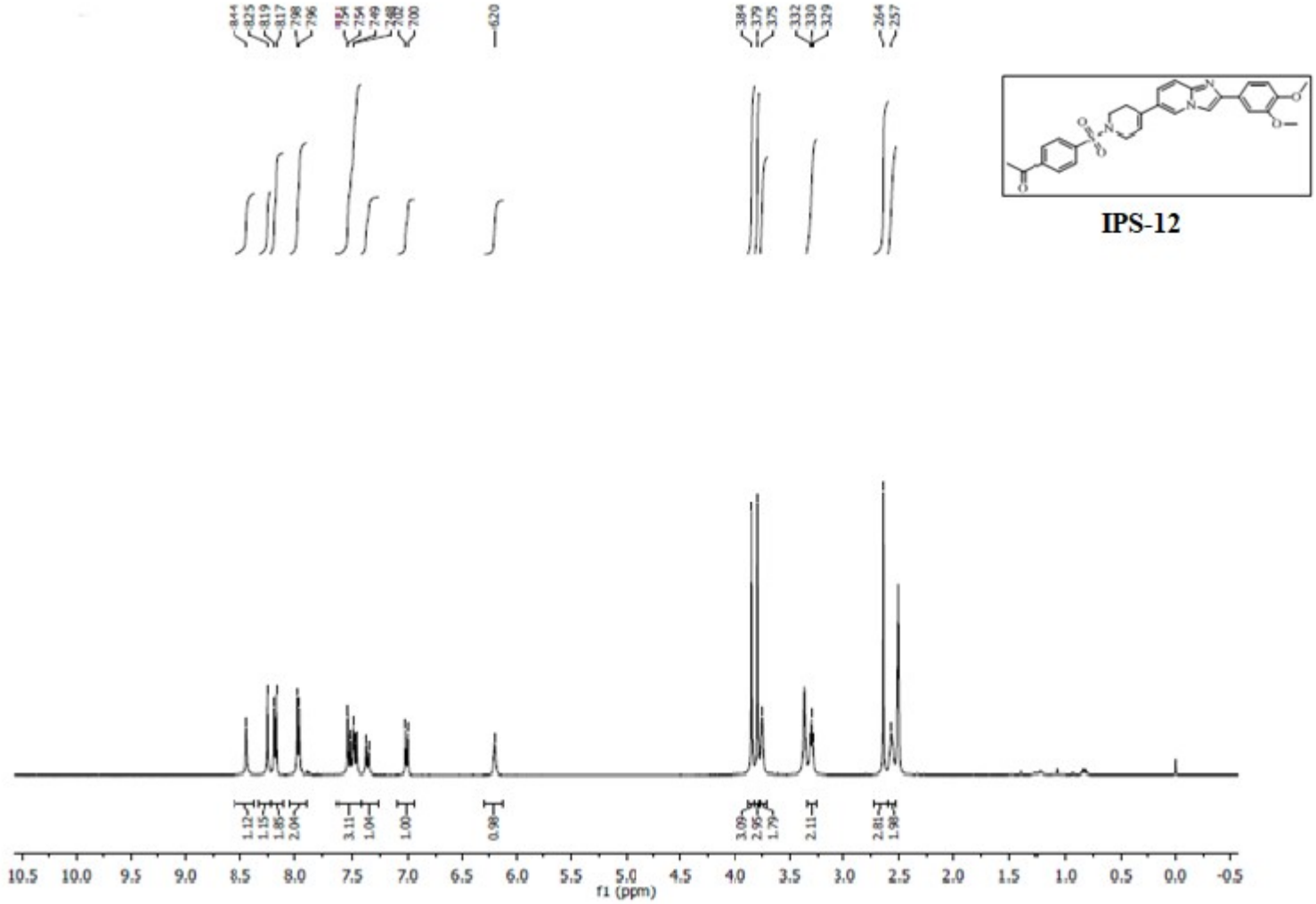

^{1}H NMR spectrum of compound **IPS-12**

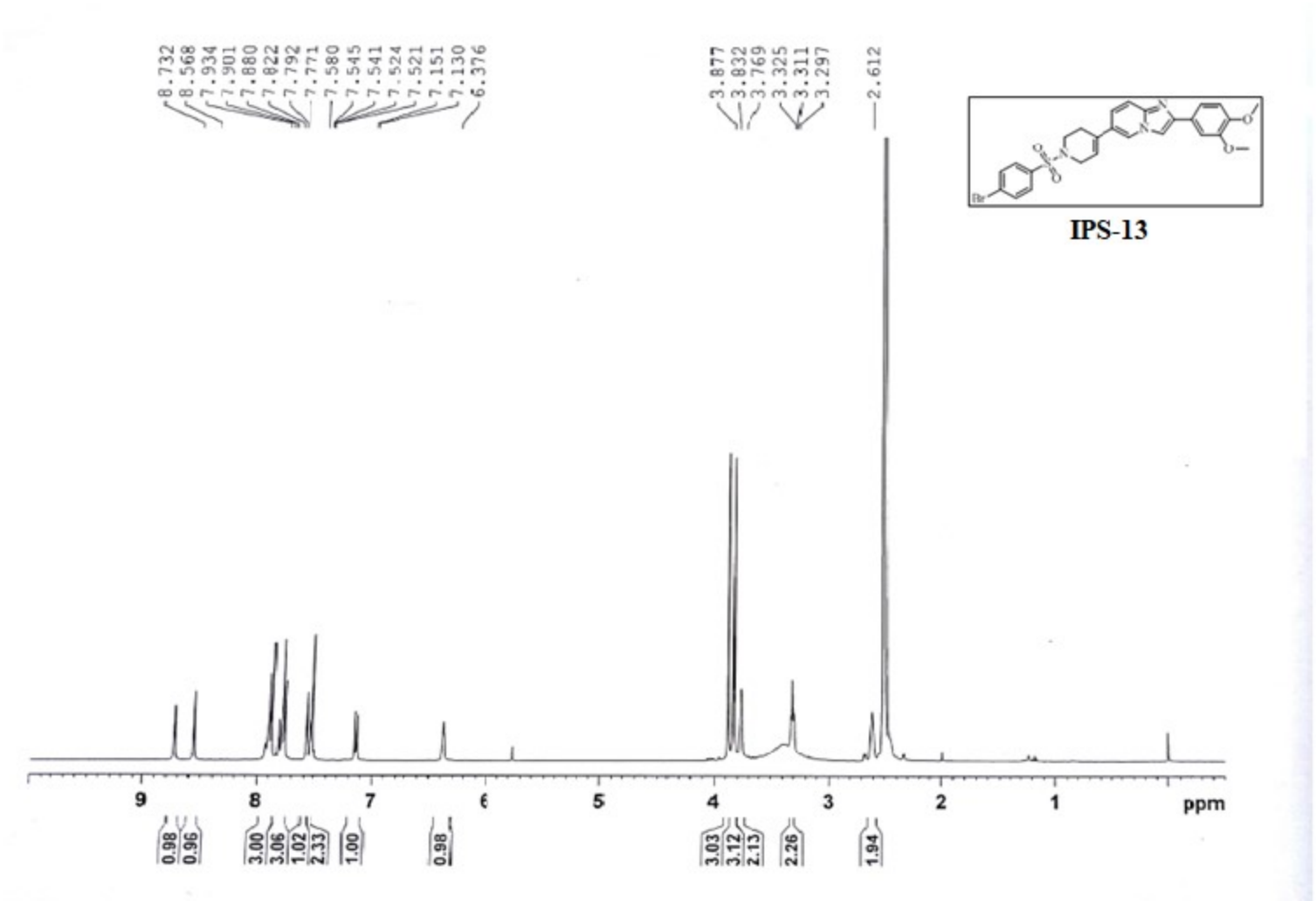

^{1}H NMR spectrum of compound **IPS-13**

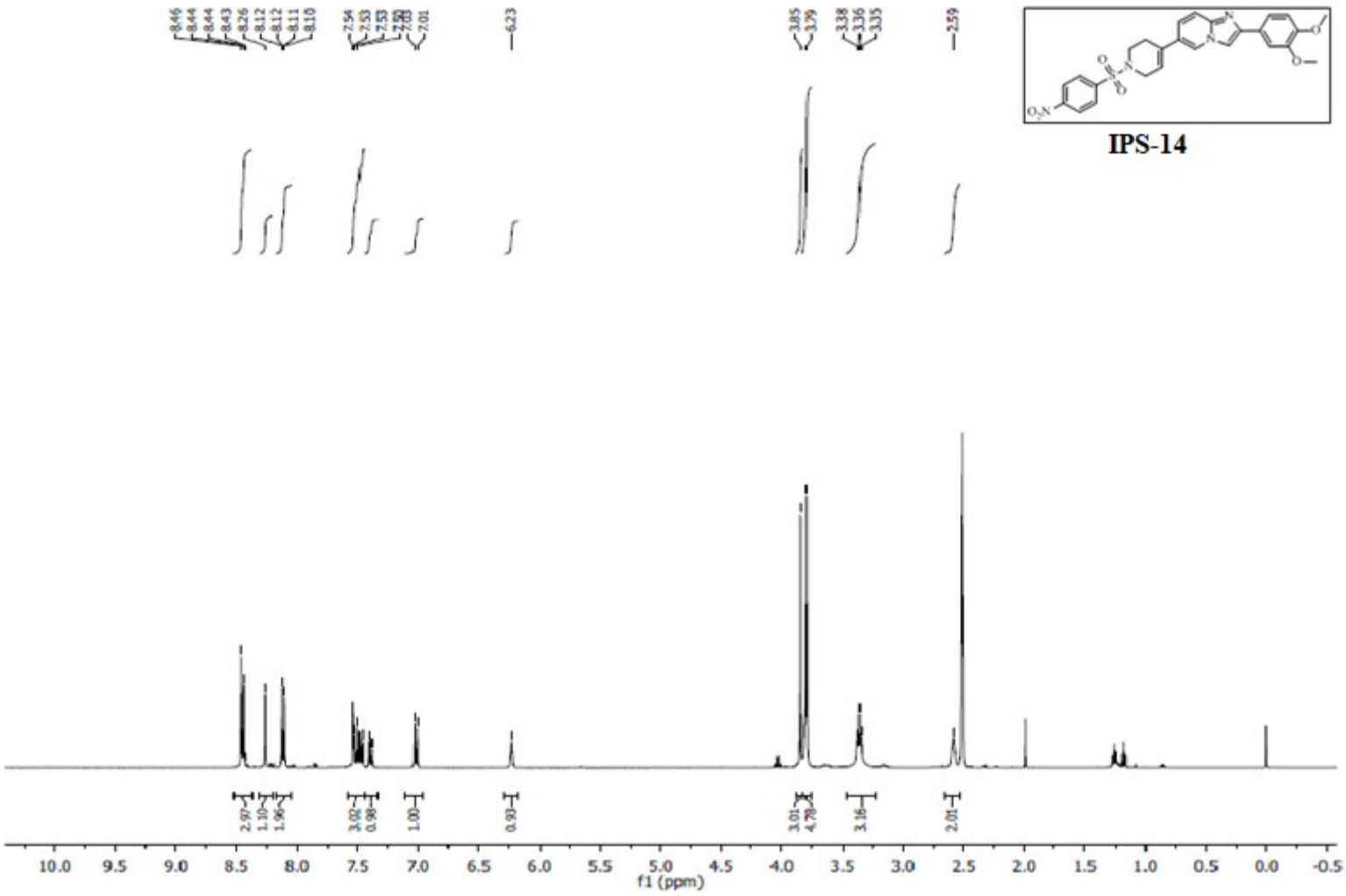

^{1}H NMR spectrum of compound **IPS-14**

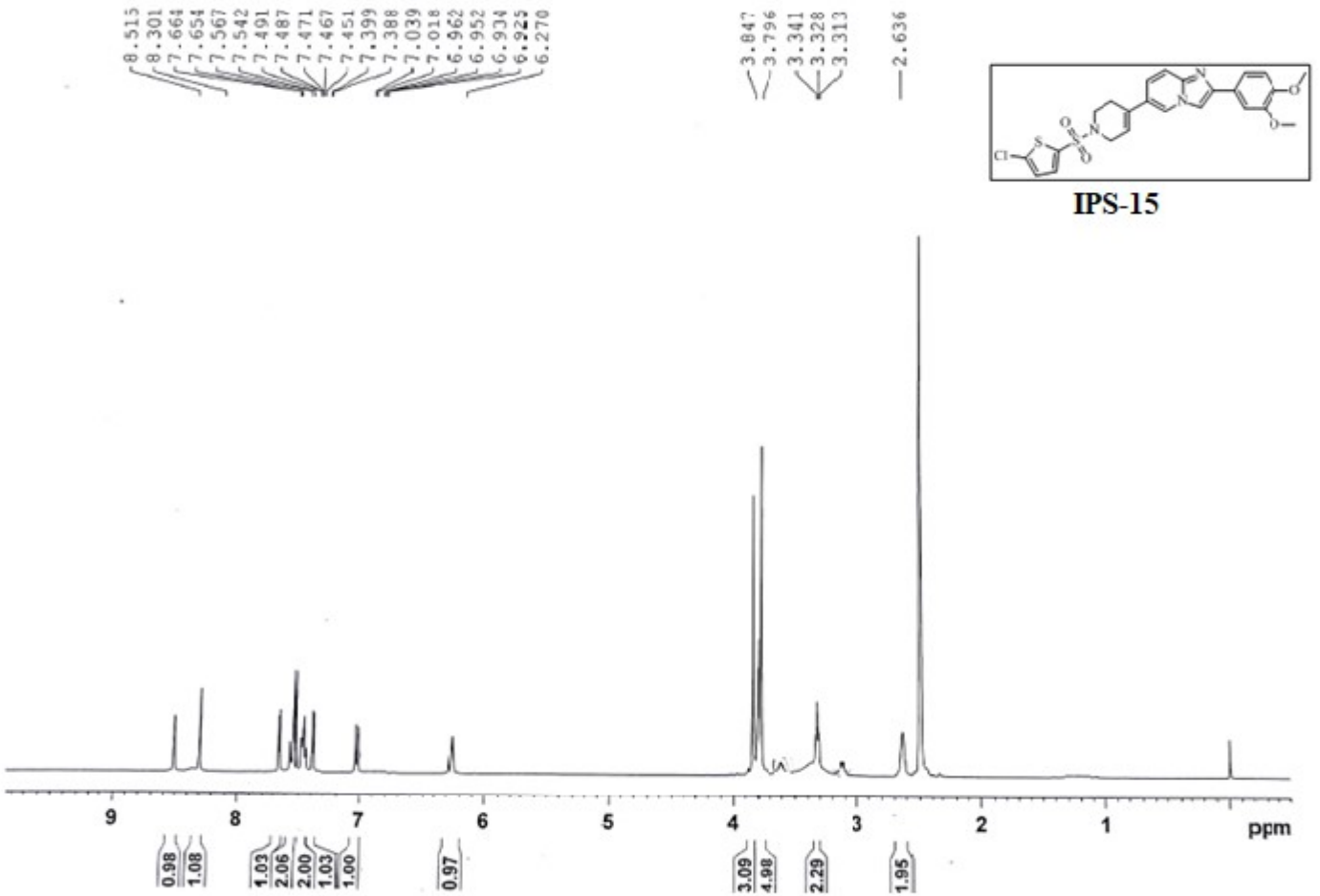

^{1}H NMR spectrum of compound **IPS-15**

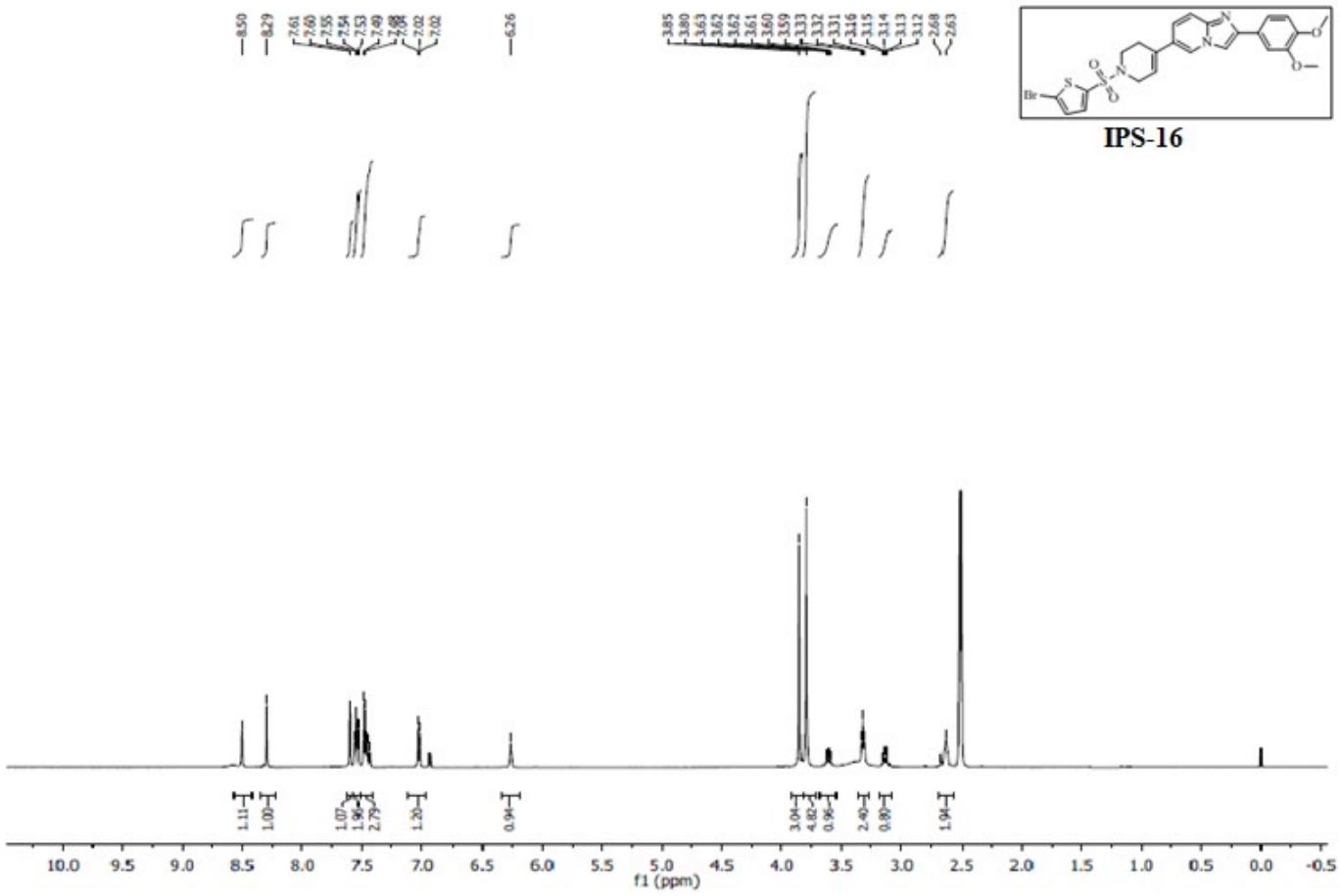

^{1}H NMR spectrum of compound **IPS-16**

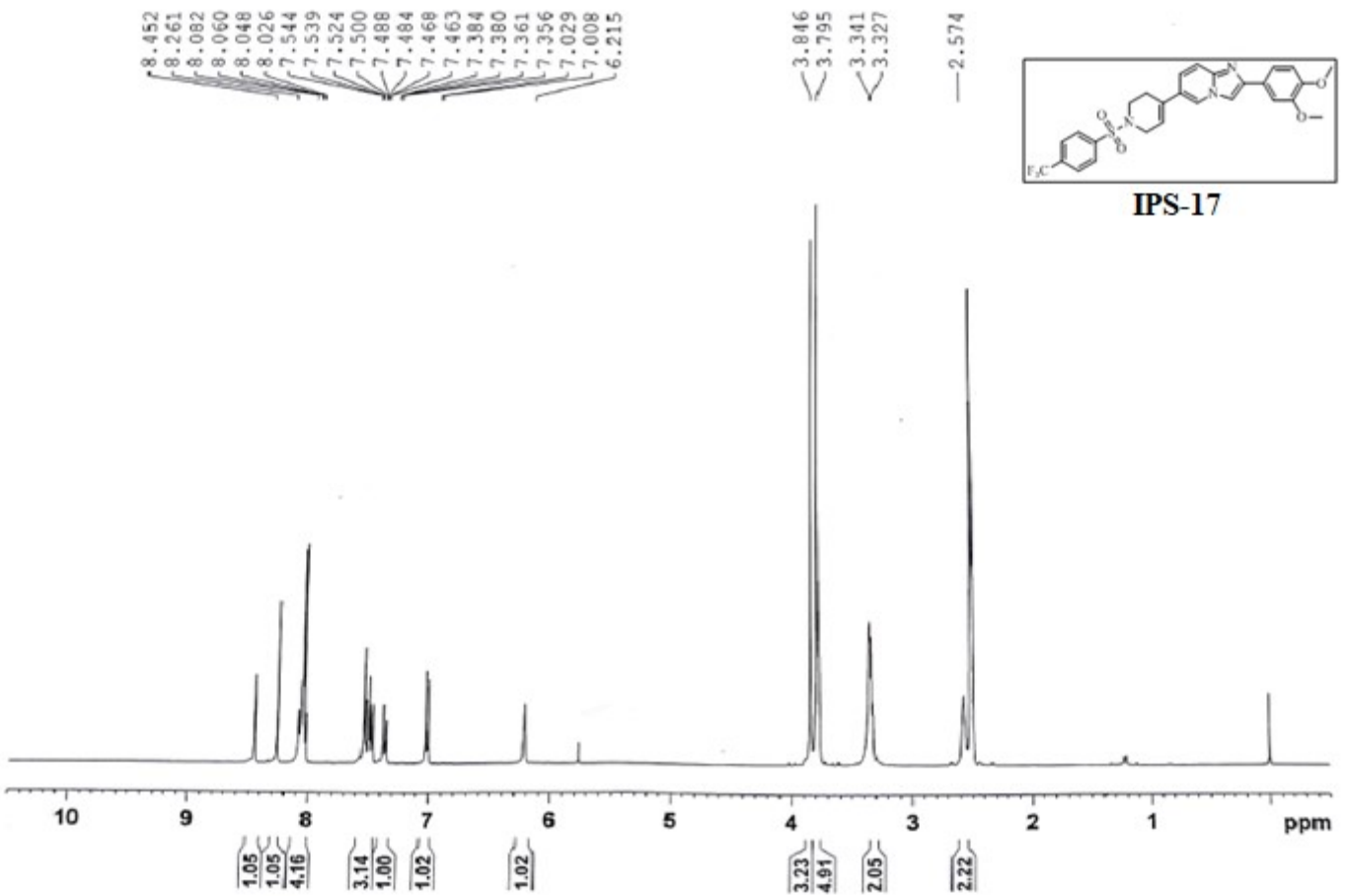

^{1}H NMR spectrum of compound **IPS-17**

^{13}C NMR spectral data for IPA and IPS series compounds

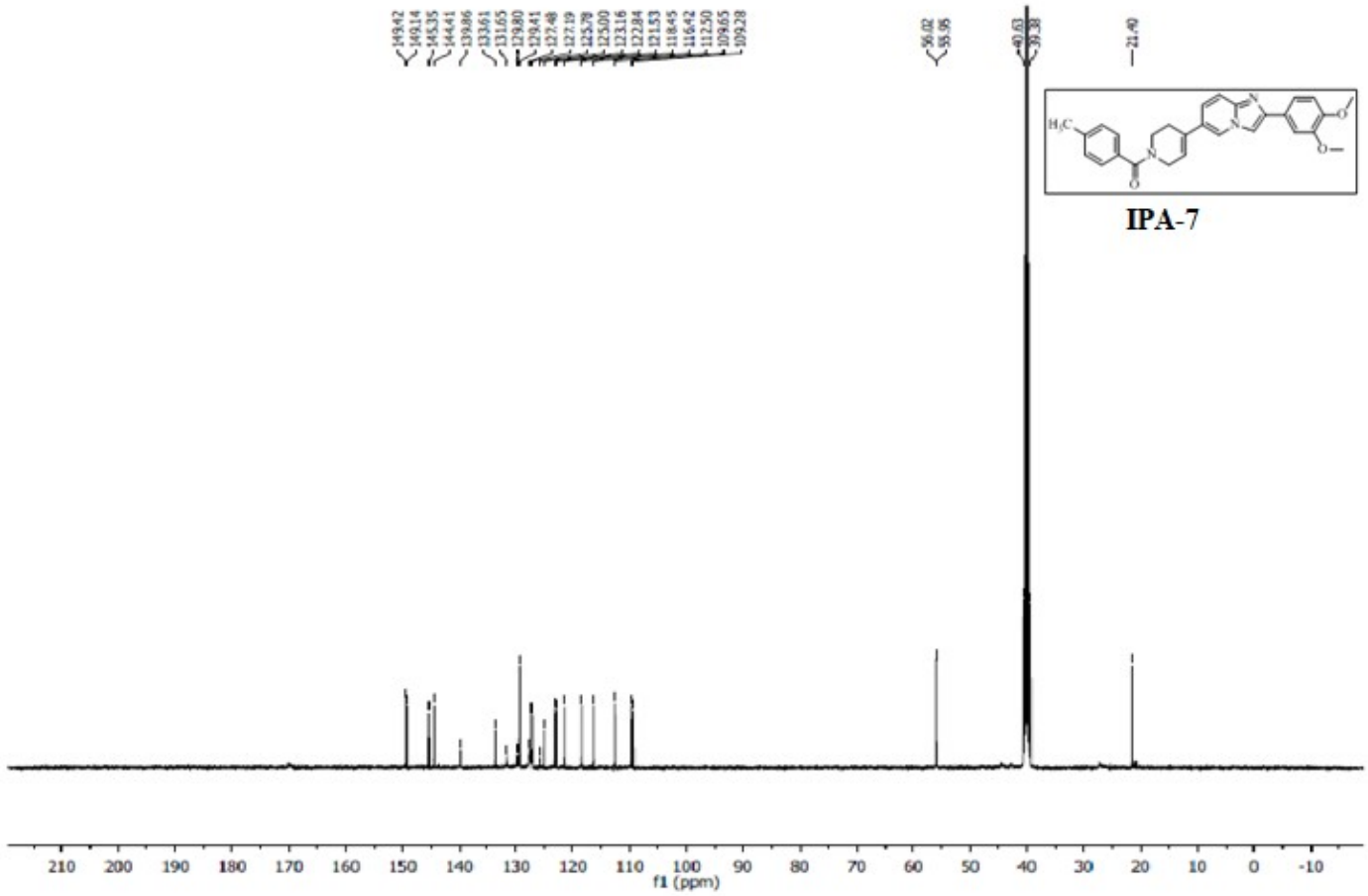

^{13}C NMR spectrum of compound **IPA-7**

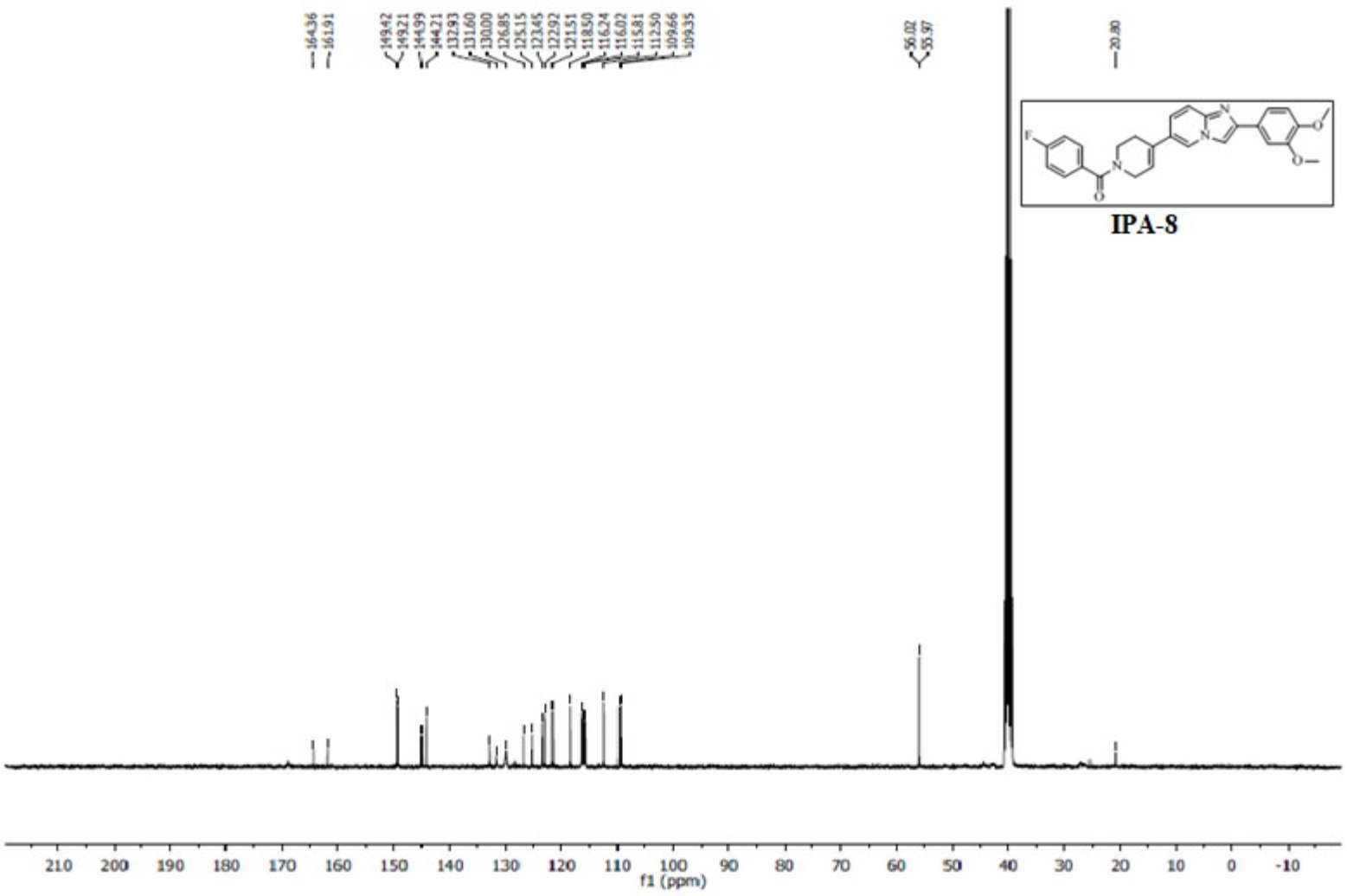

^{13}C NMR spectrum of compound **IPA-8**

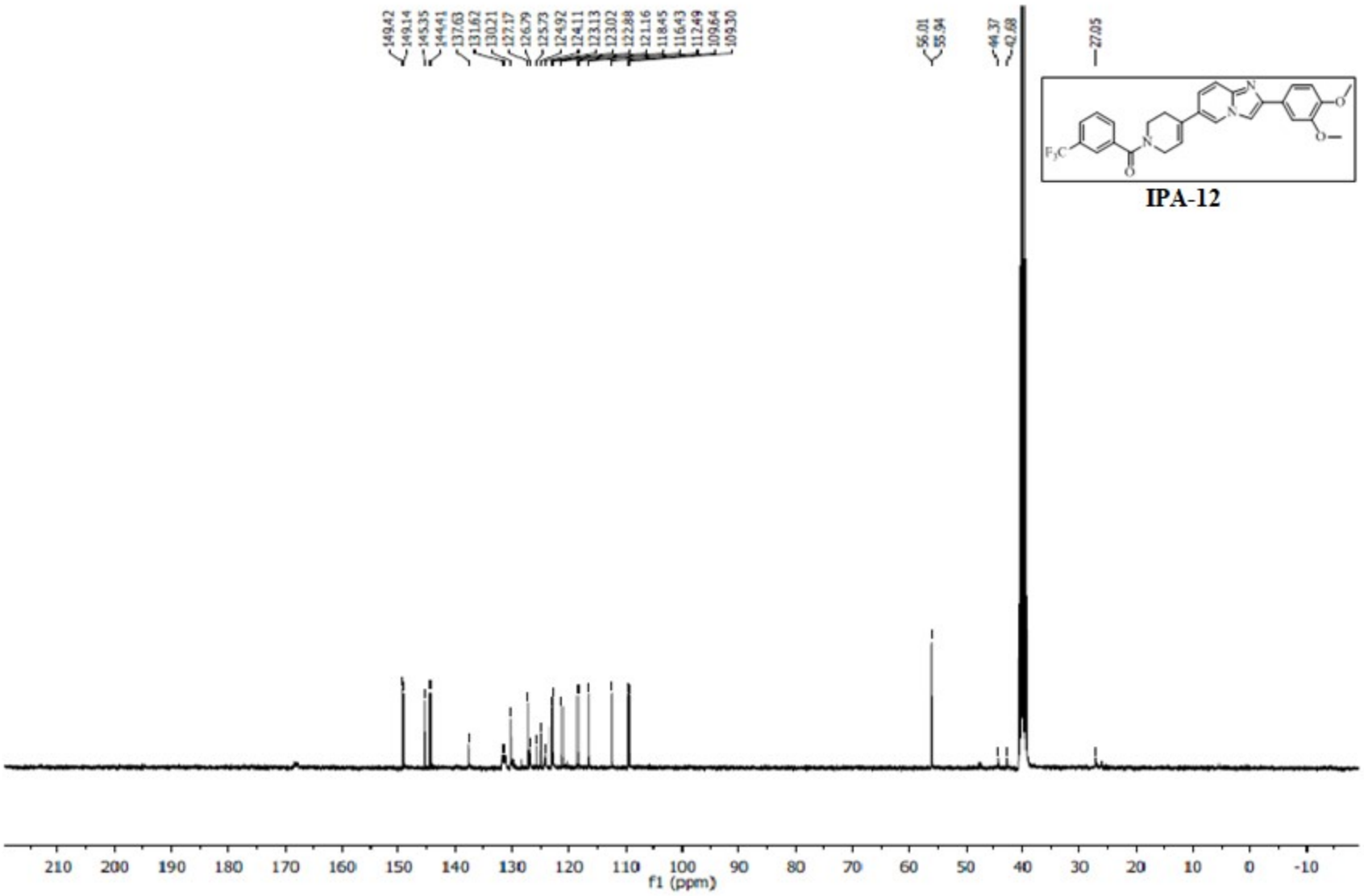

^{13}C NMR spectrum of compound **IPA-12**

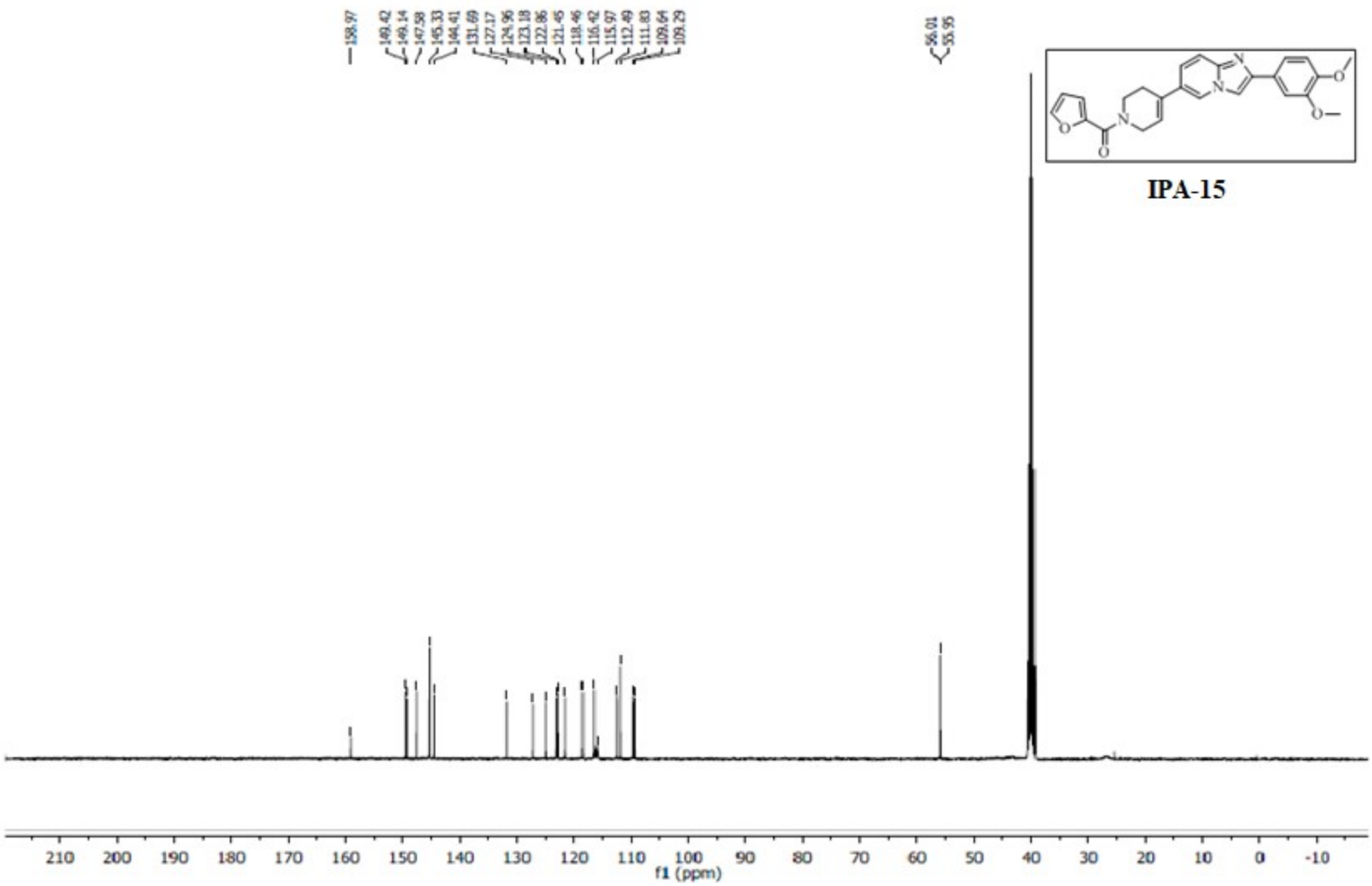

^{13}C NMR spectrum of compound **IPA-15**

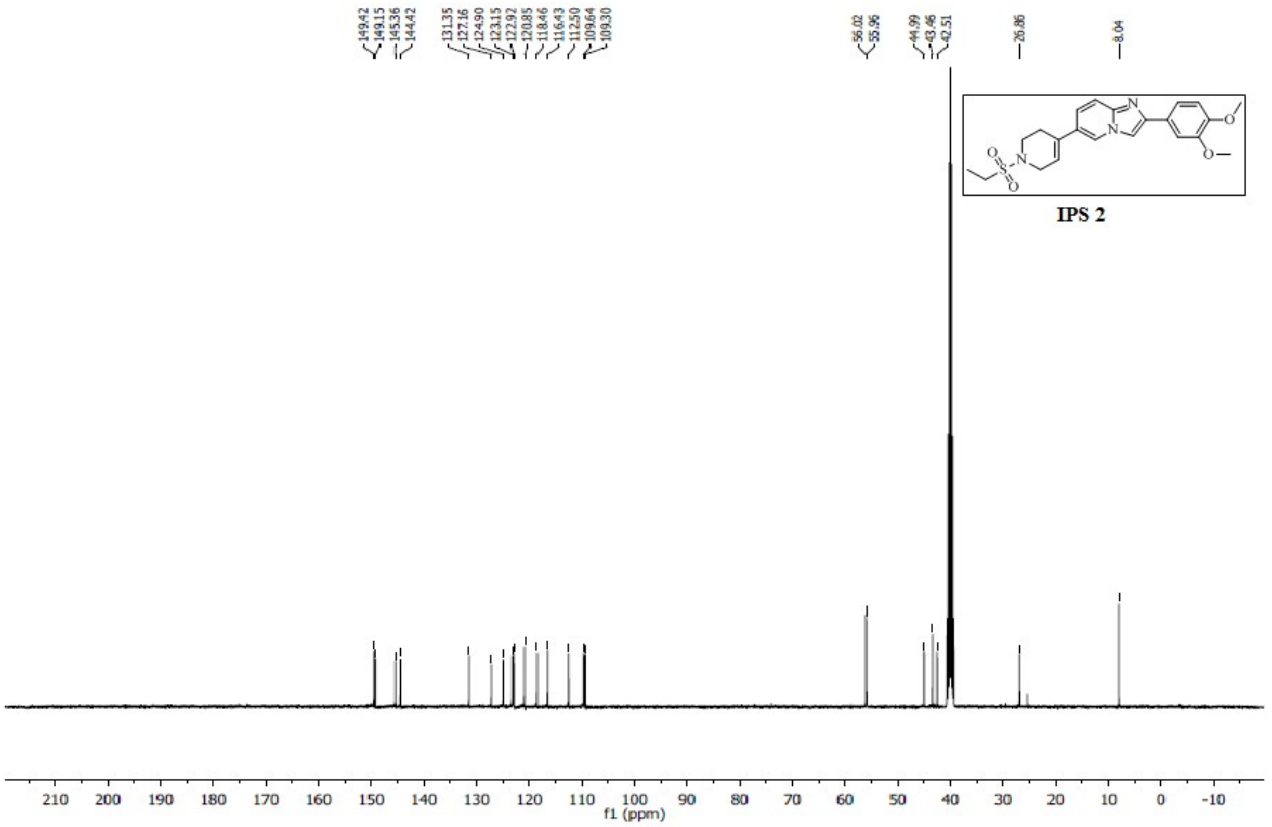

^{13}C NMR spectrum of compound **IPS-2**

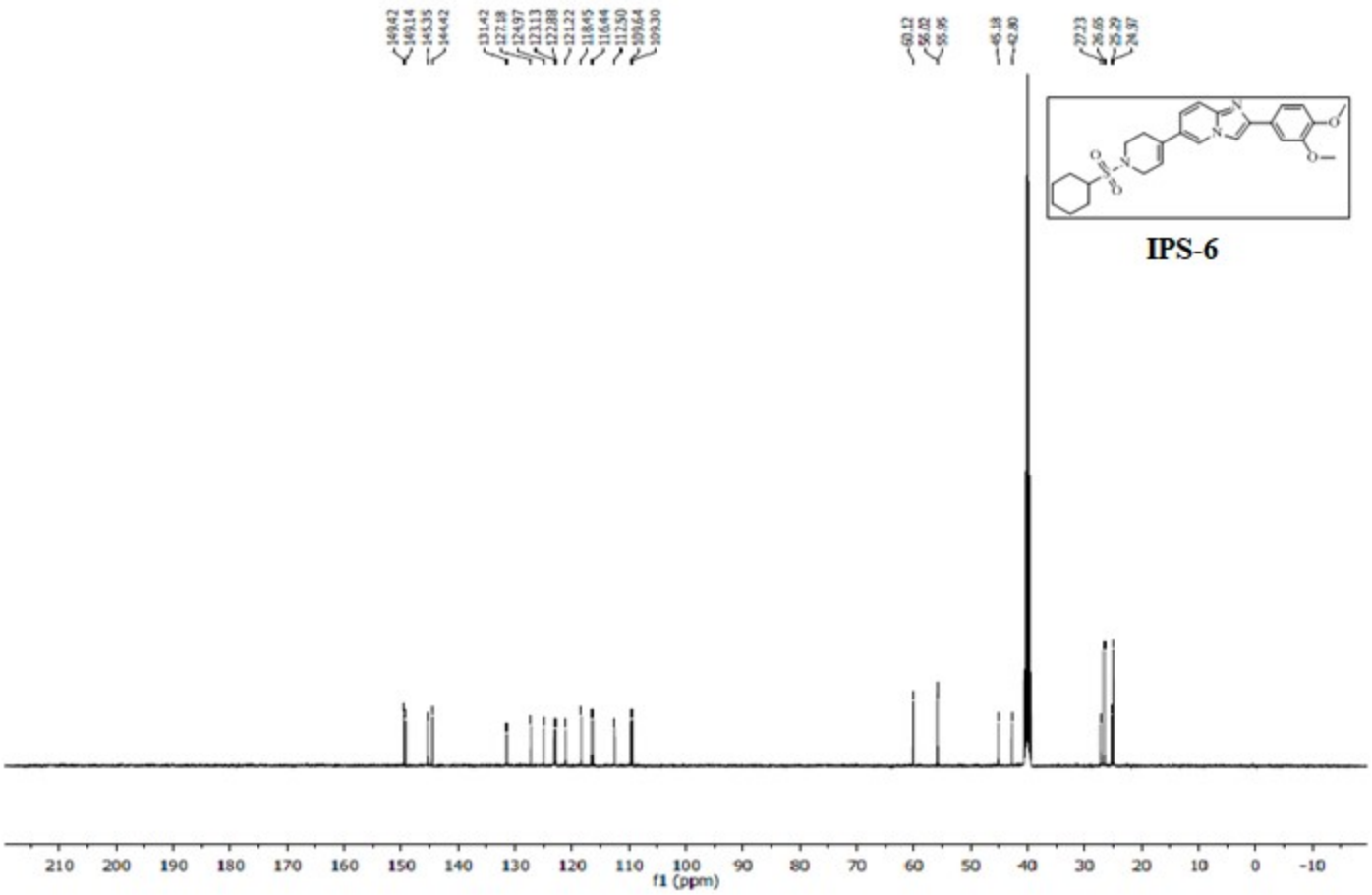

^{13}C NMR spectrum of compound **IPS-6**

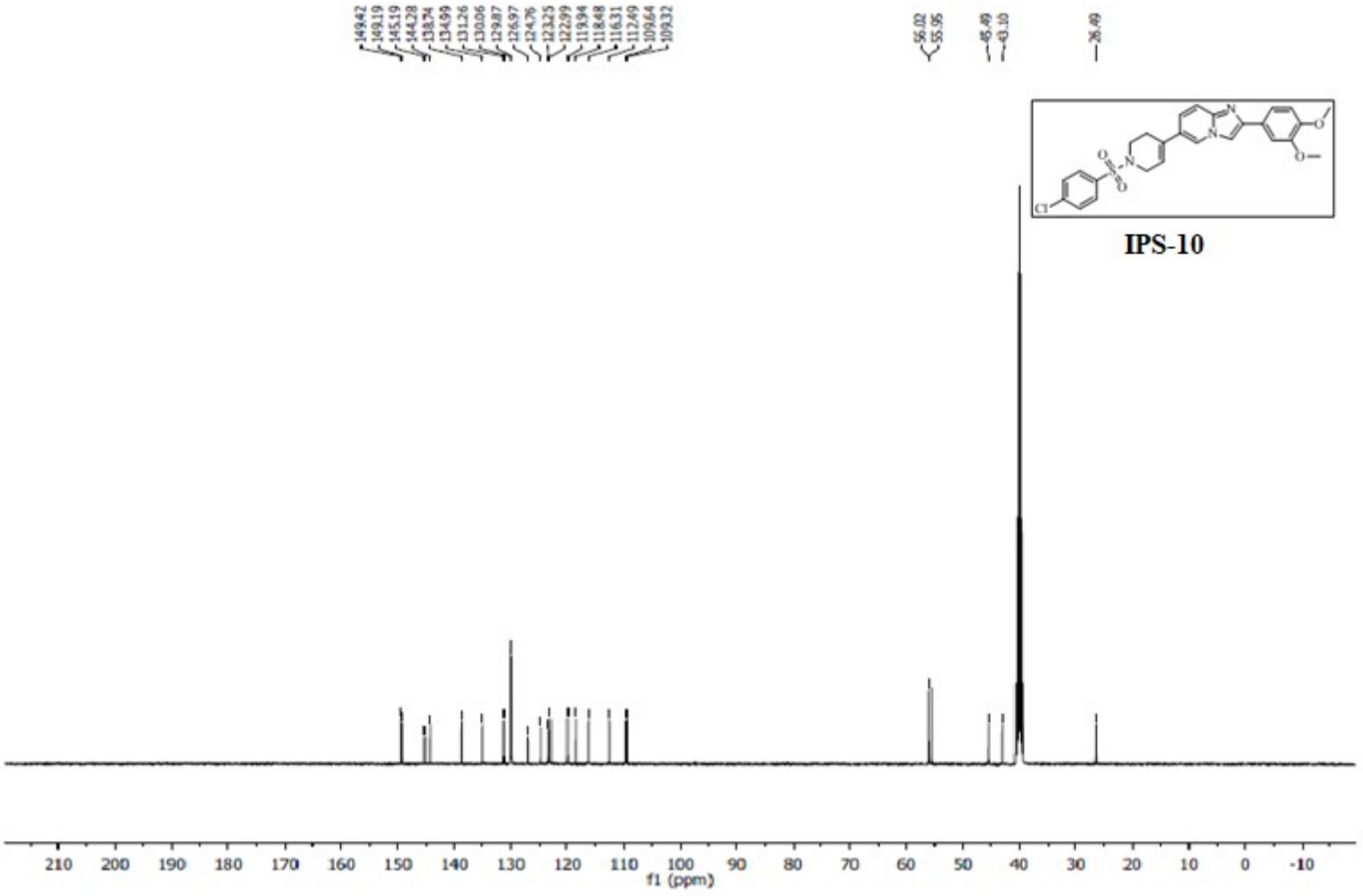

^{13}C NMR spectrum of compound **IPS-10**

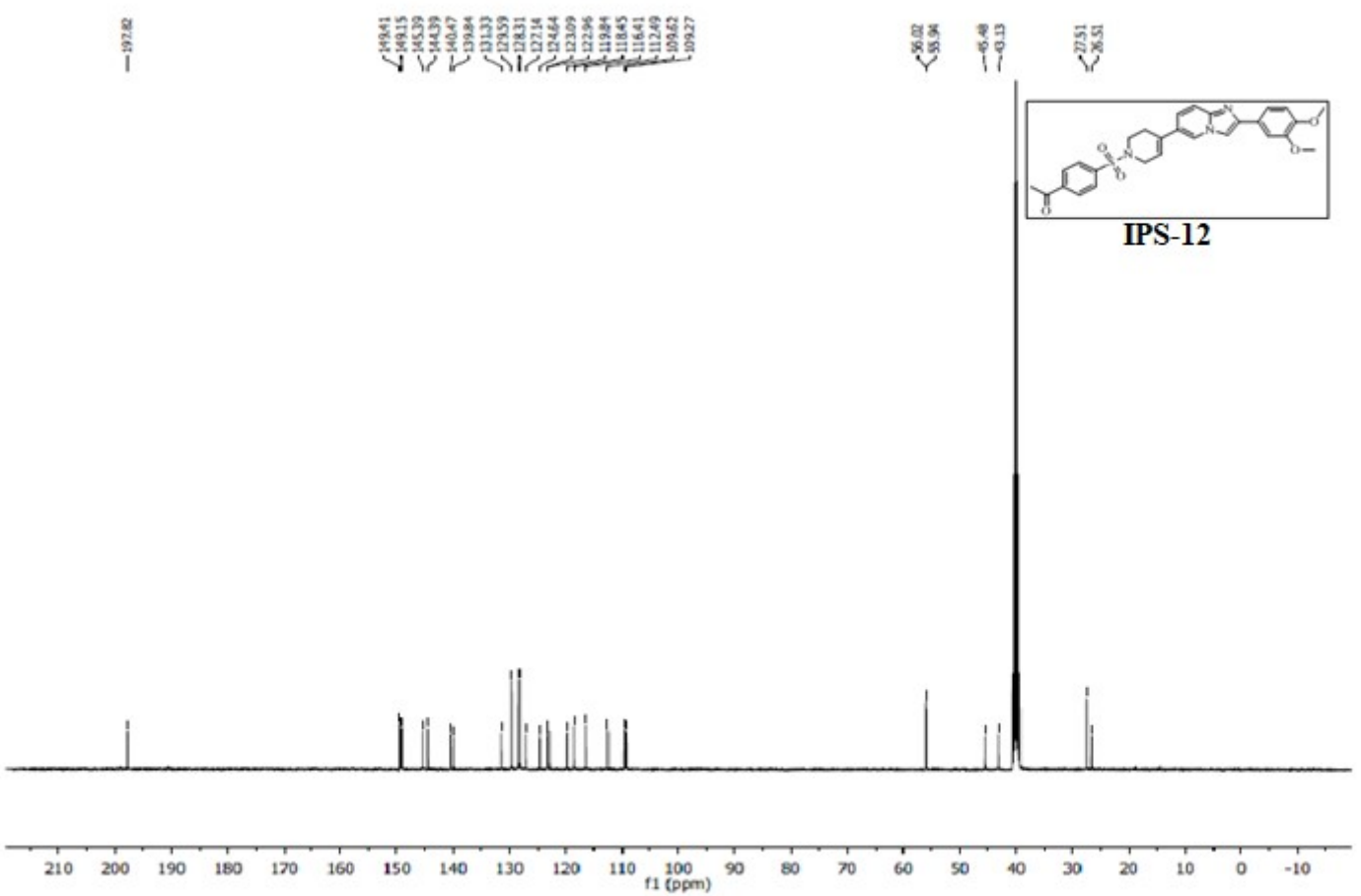

^{13}C NMR spectrum of compound **IPS-12**

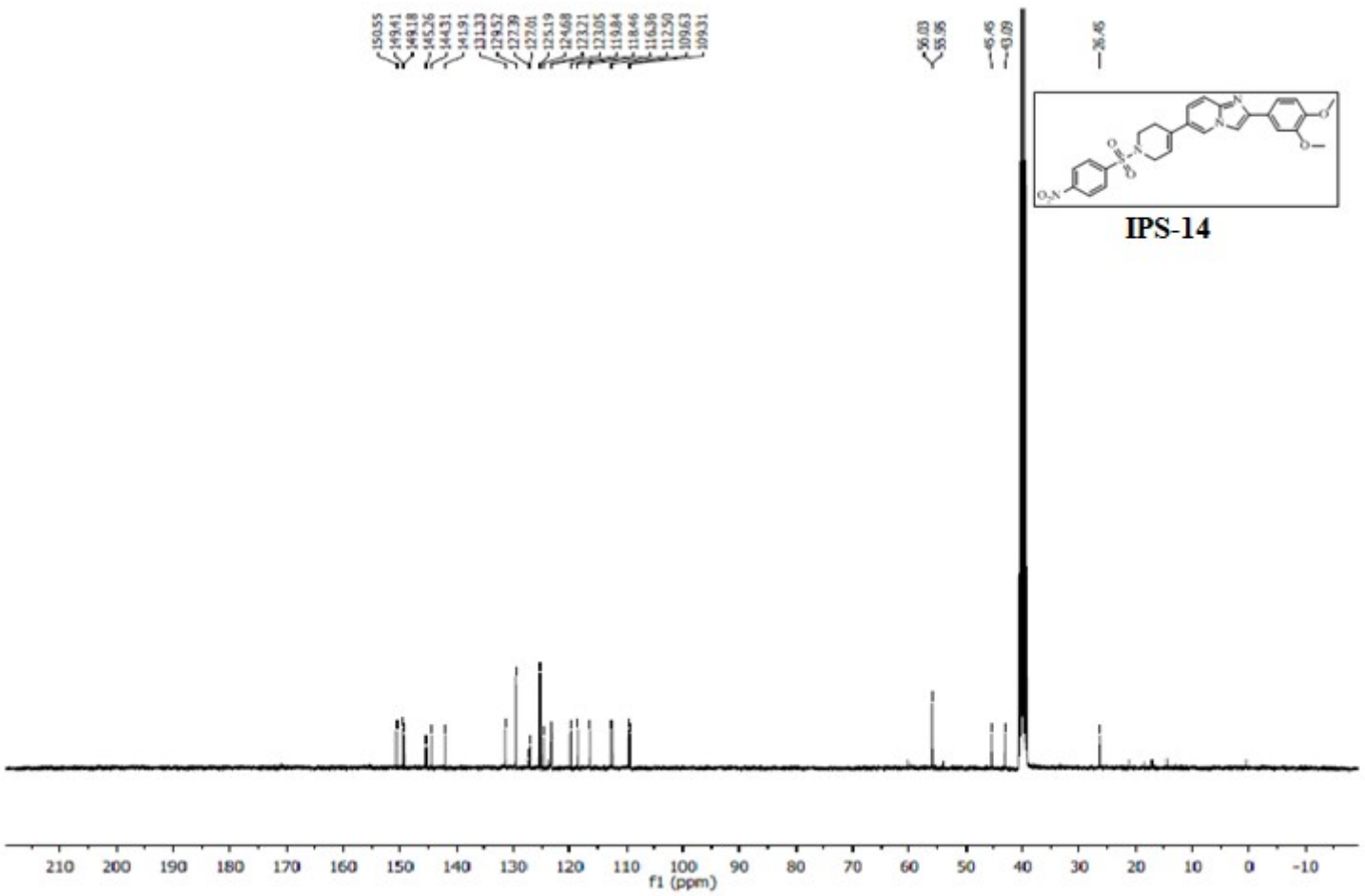

^{13}C NMR spectrum of compound **IPS-14**

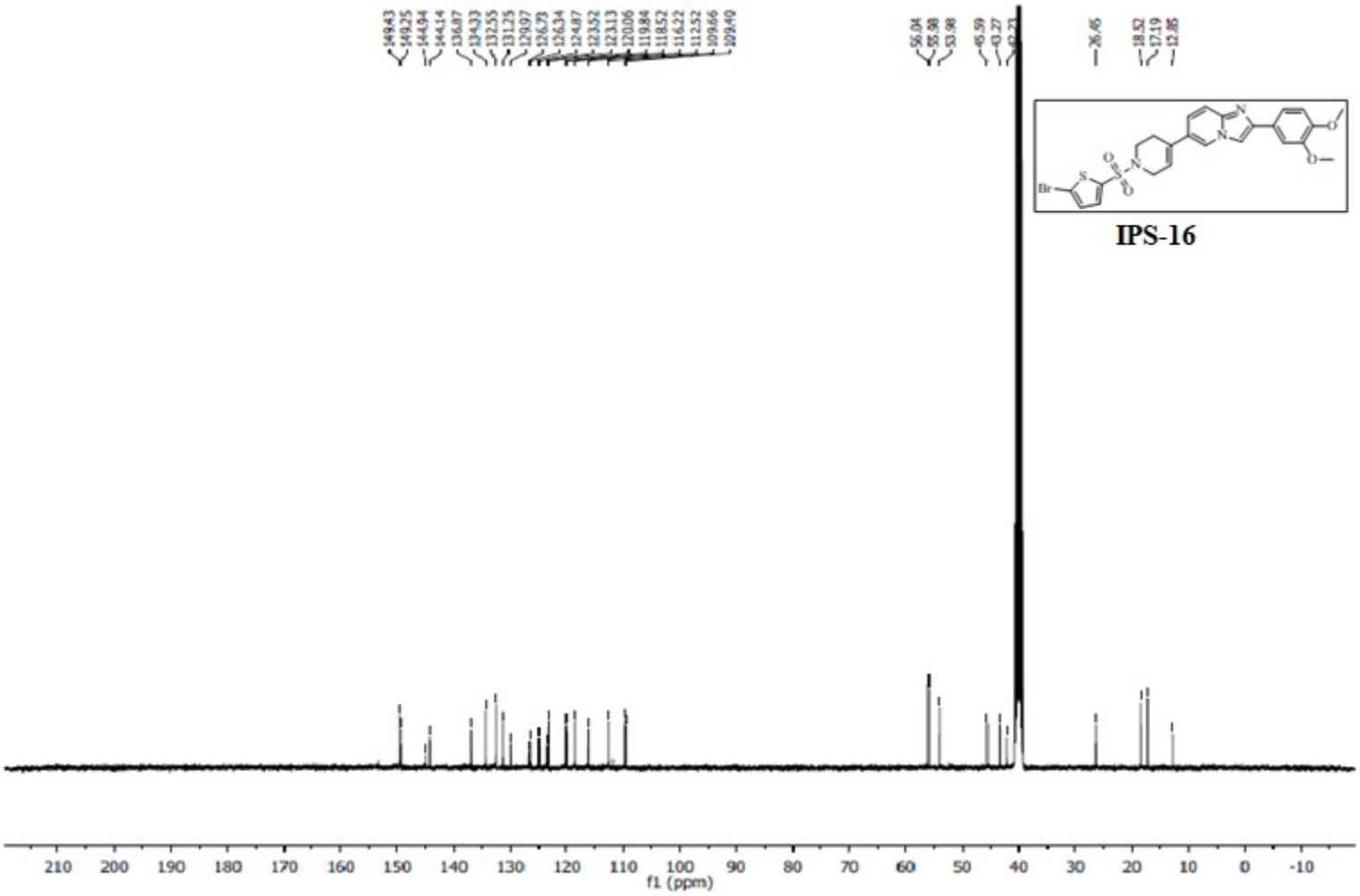

^{13}C NMR spectrum of compound **IPS-16**

ESI MS spectral data for IPA and IPS series compounds

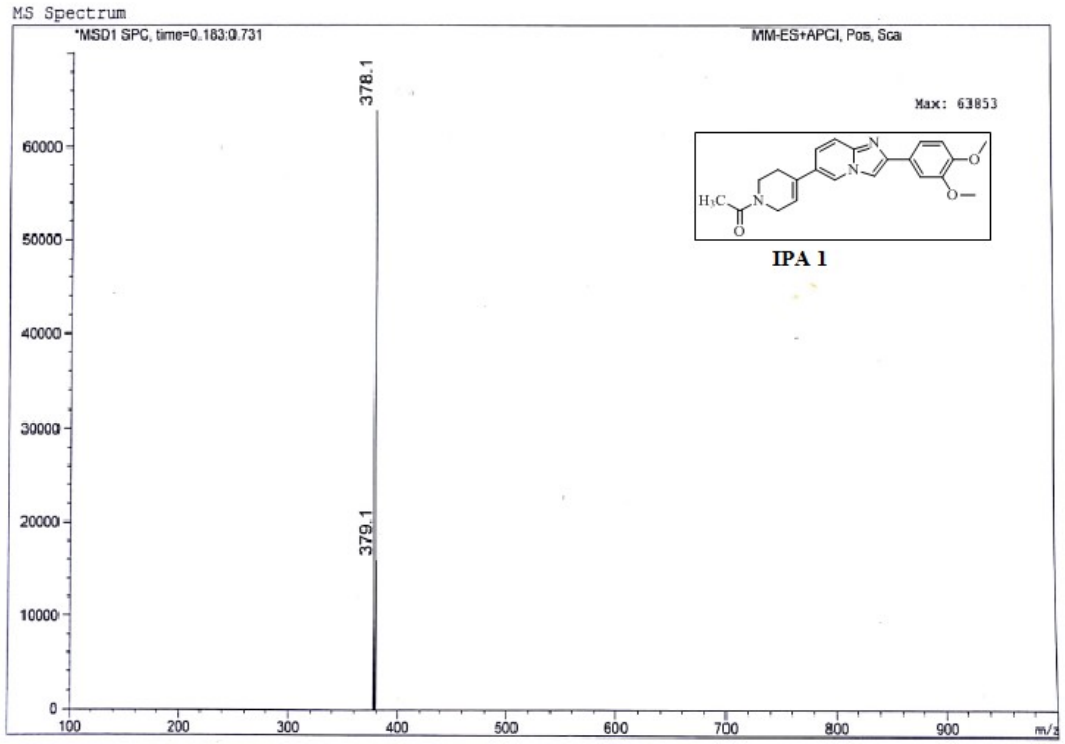

ESI MS spectrum of compound **IPA-1**

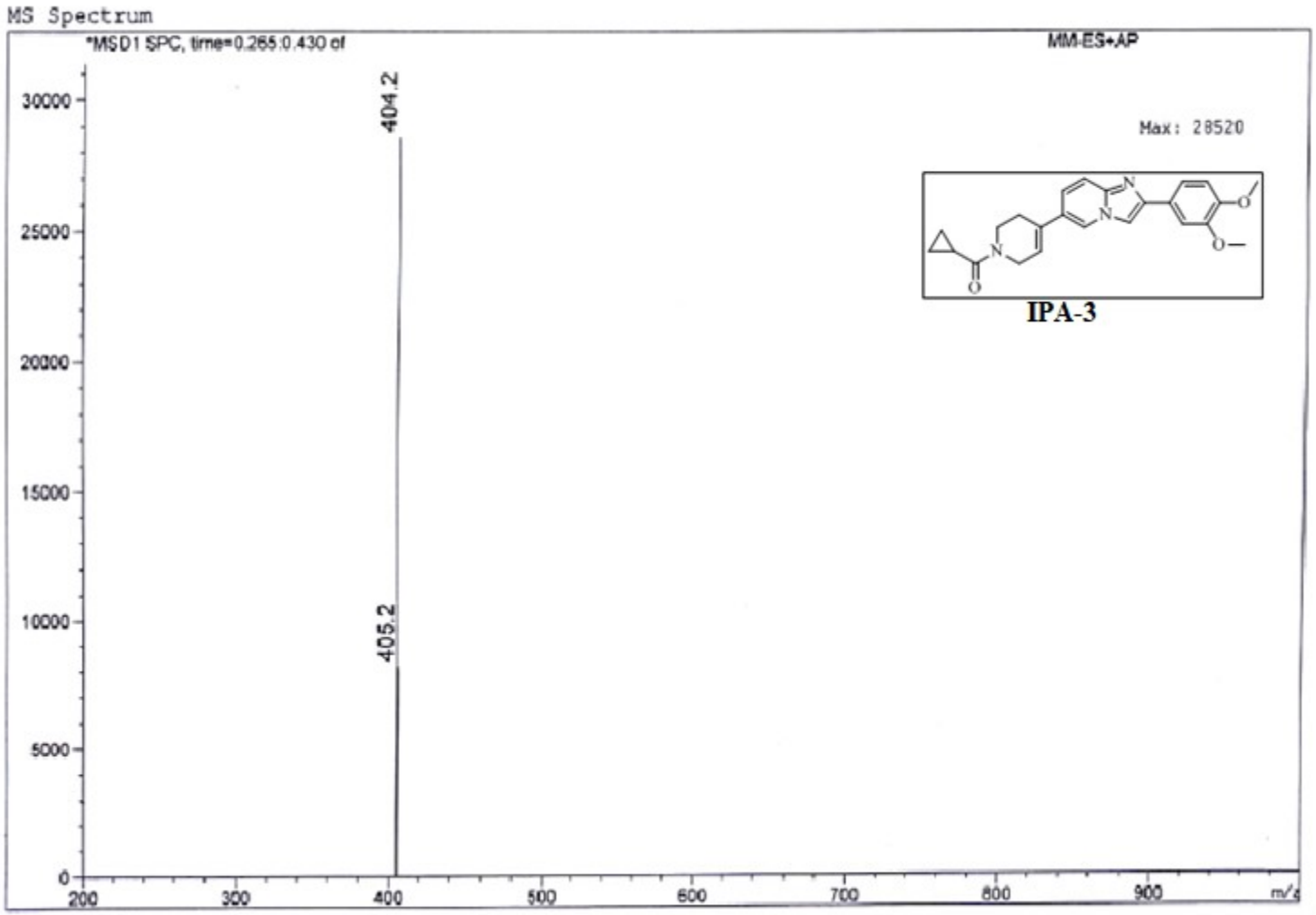

ESI MS spectrum of compound **IPA-3**

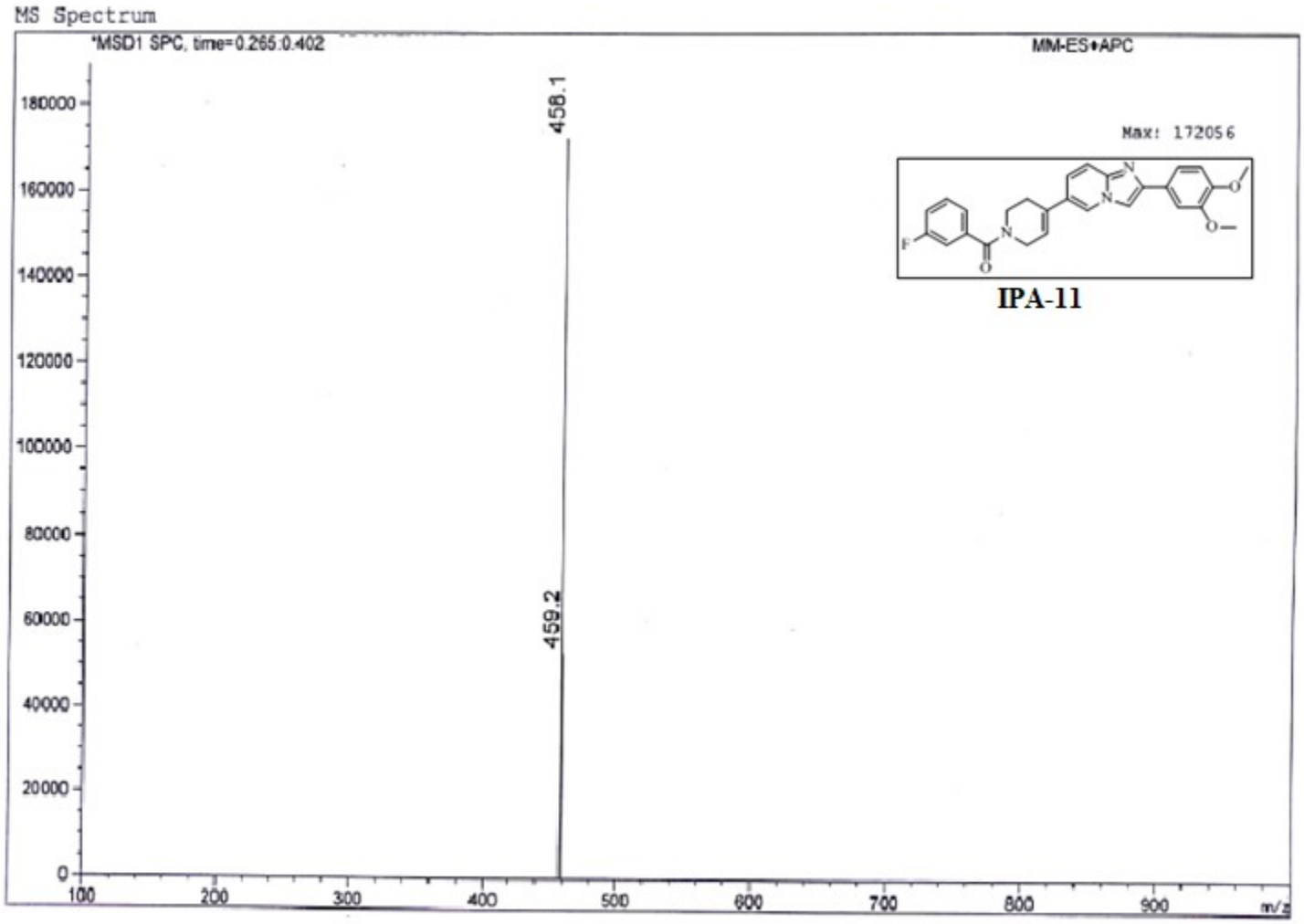

ESI MS spectrum of compound **IPA-11**

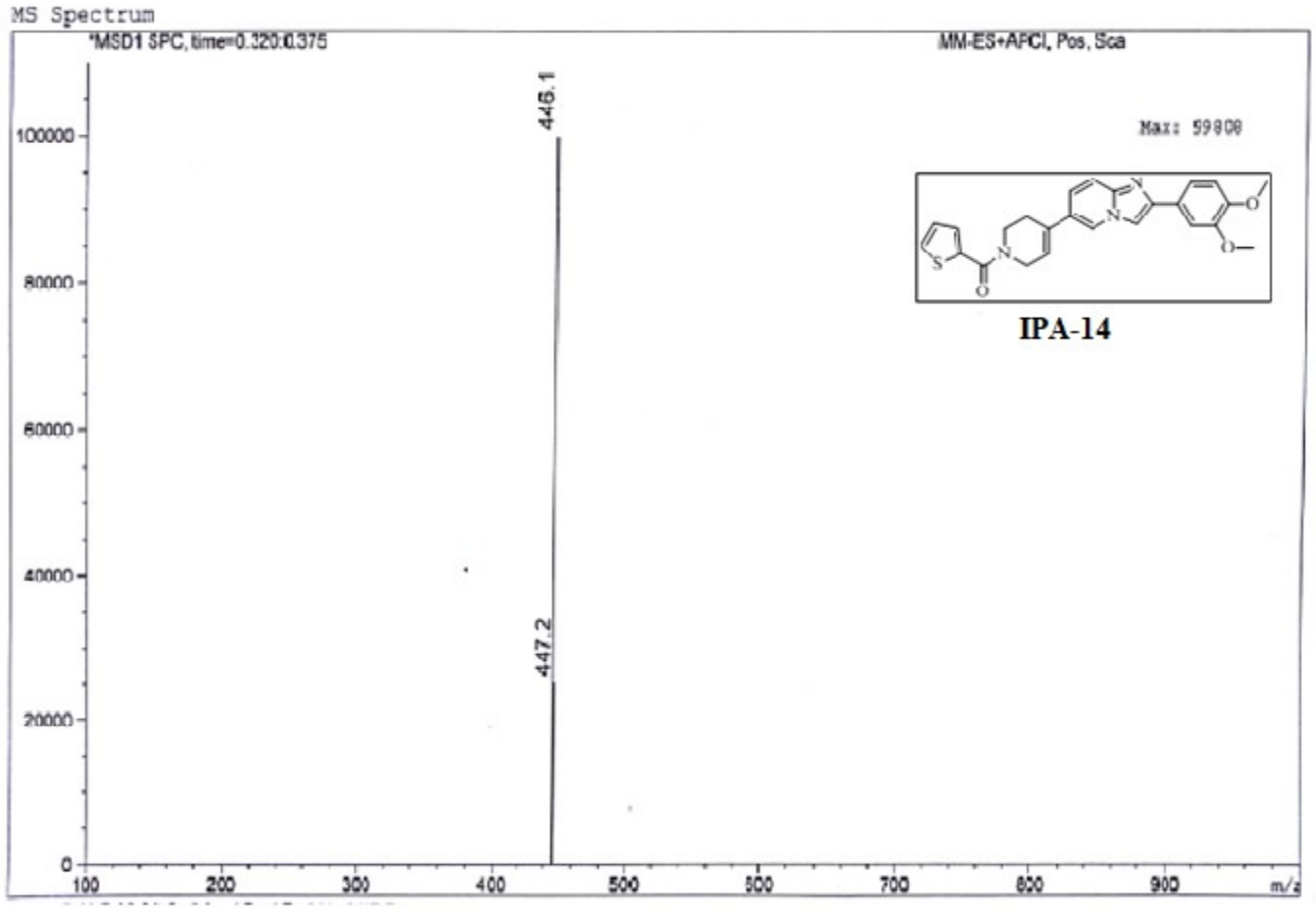

ESI MS spectrum of compound **IPA-14**

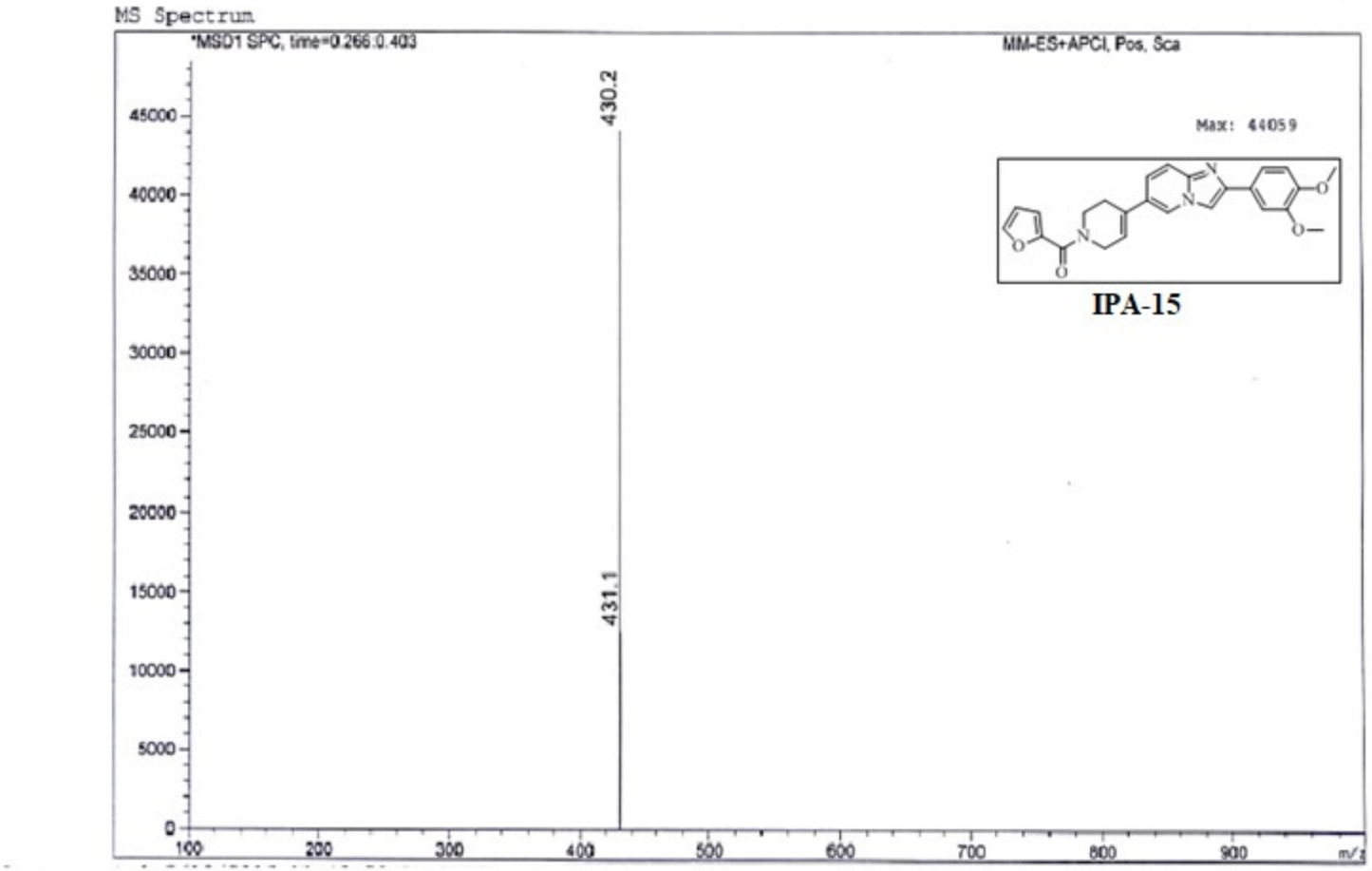

ESI MS spectrum of compound **IPA-15**

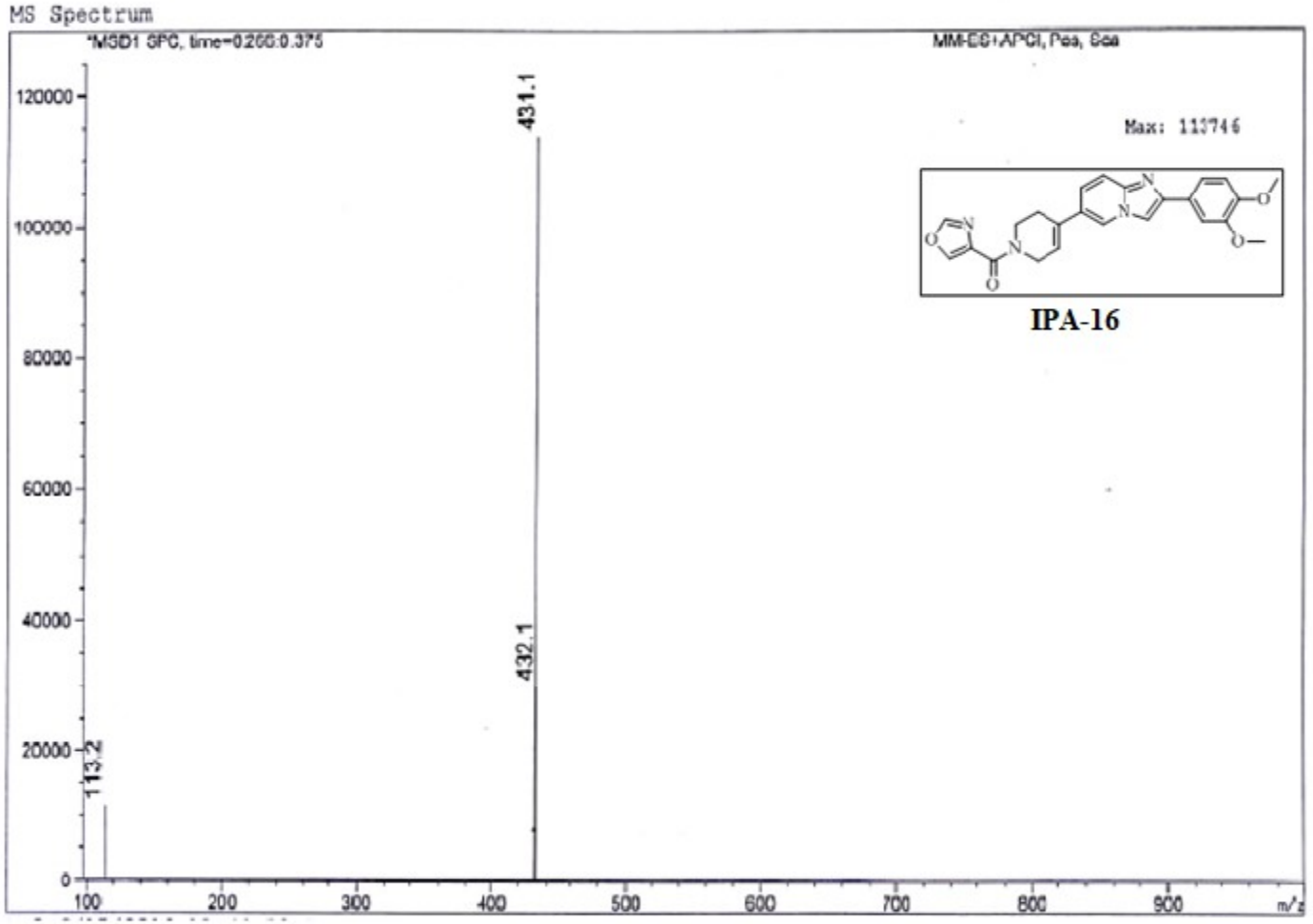

ESI MS spectrum of compound **IPA-16**

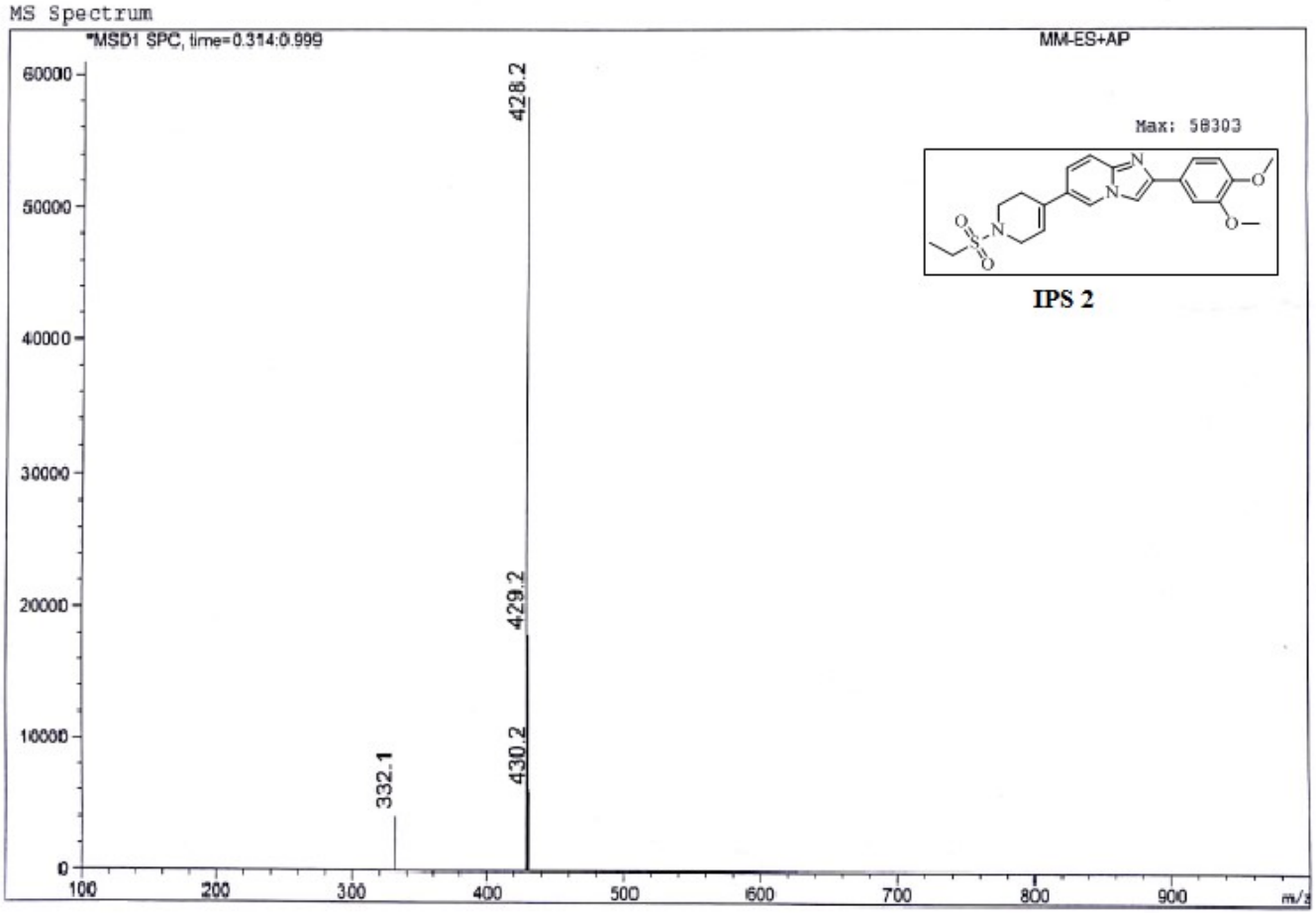

ESI MS spectrum of compound **IPS-2**

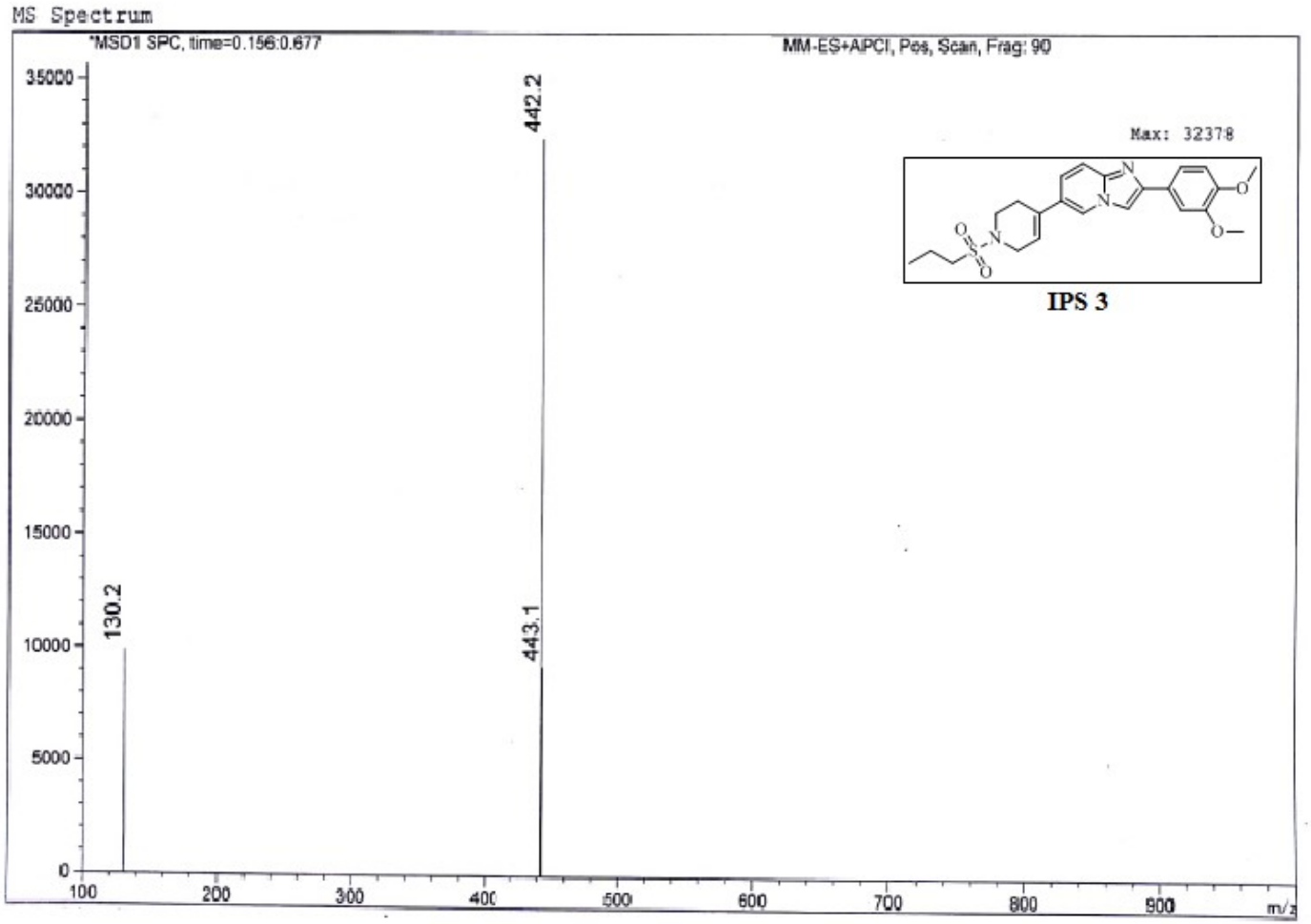

ESI MS spectrum of compound **IPS-3**

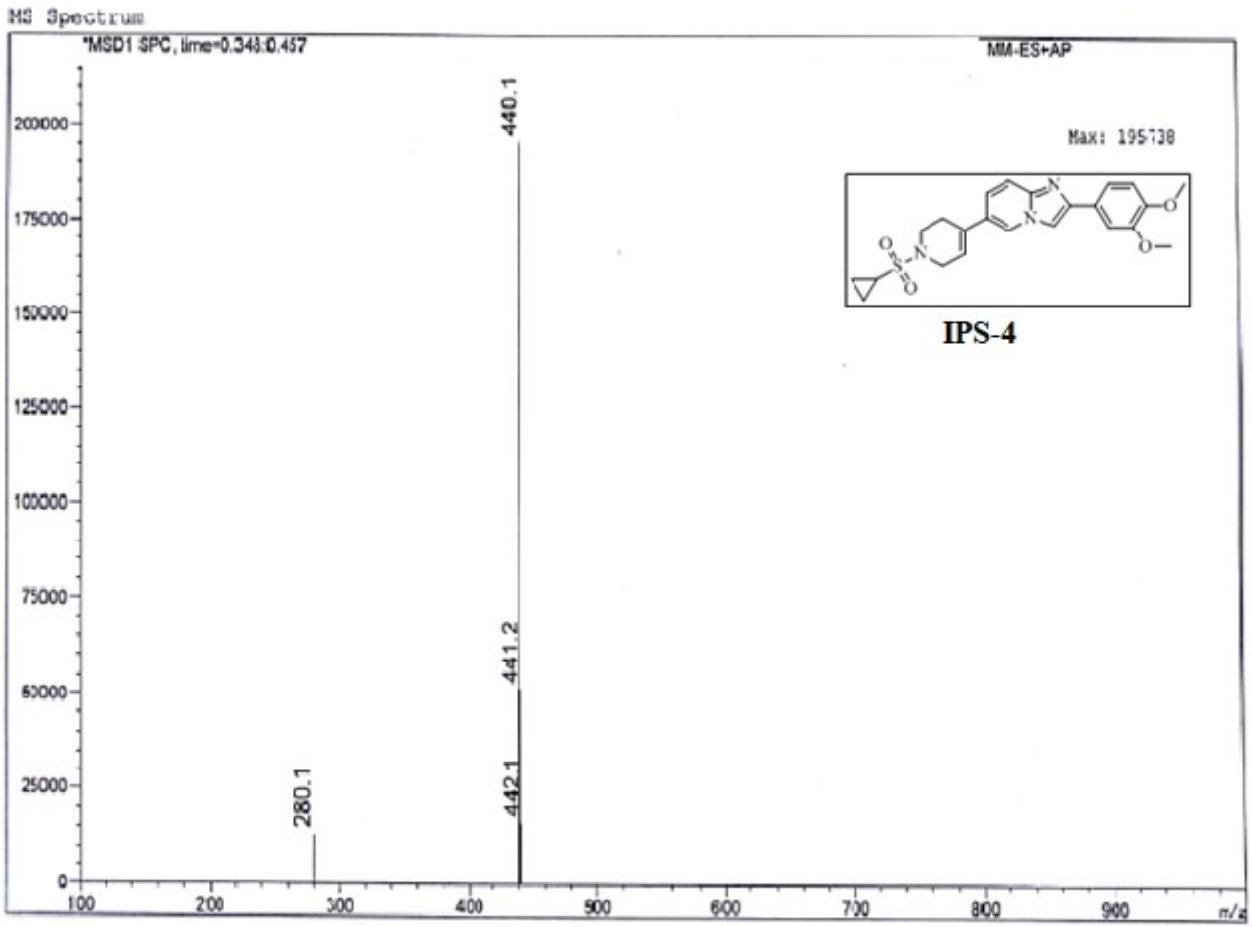

ESI MS spectrum of compound **IPS-4**

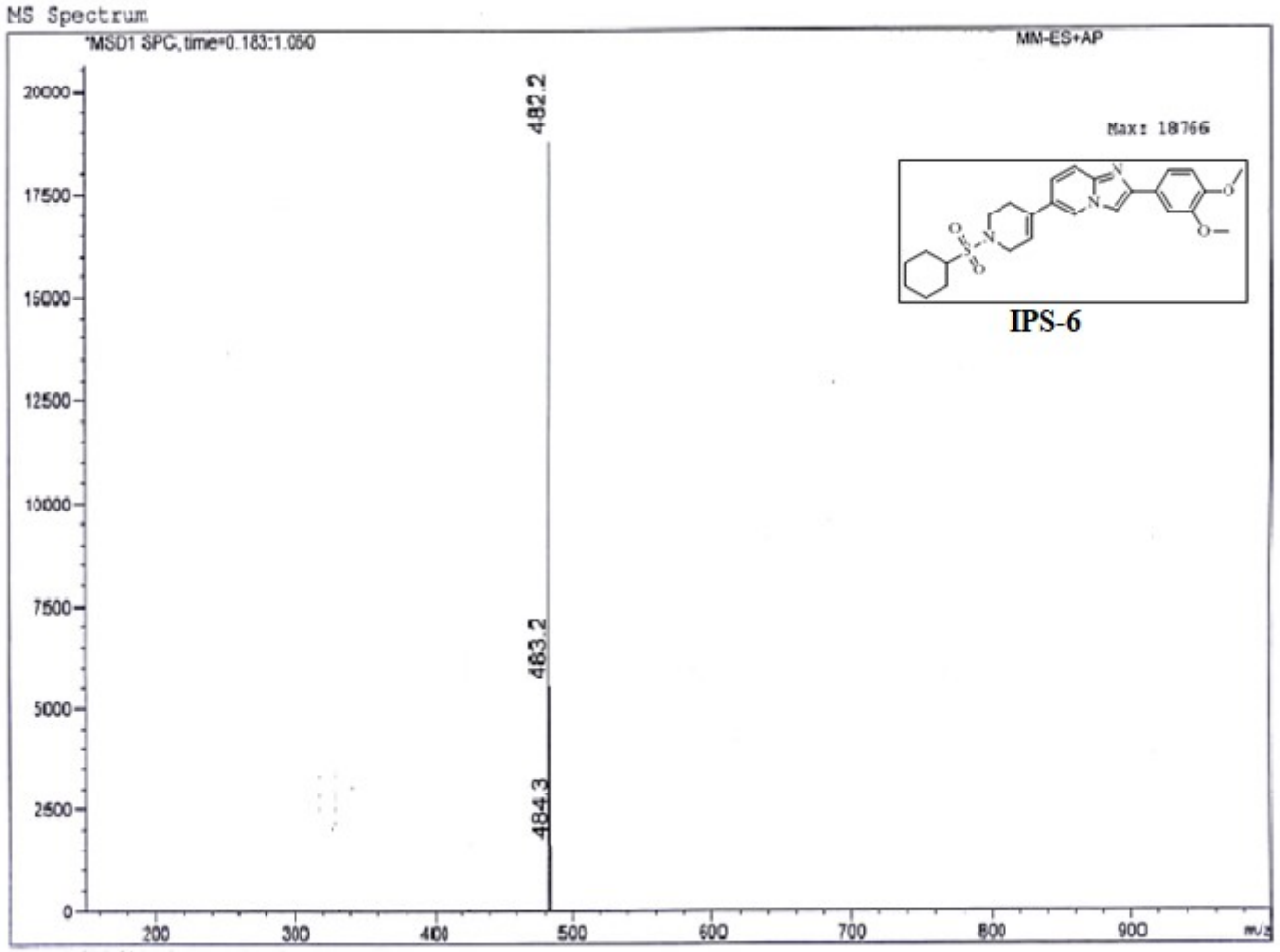

ESI MS spectrum of compound **IPS-6**

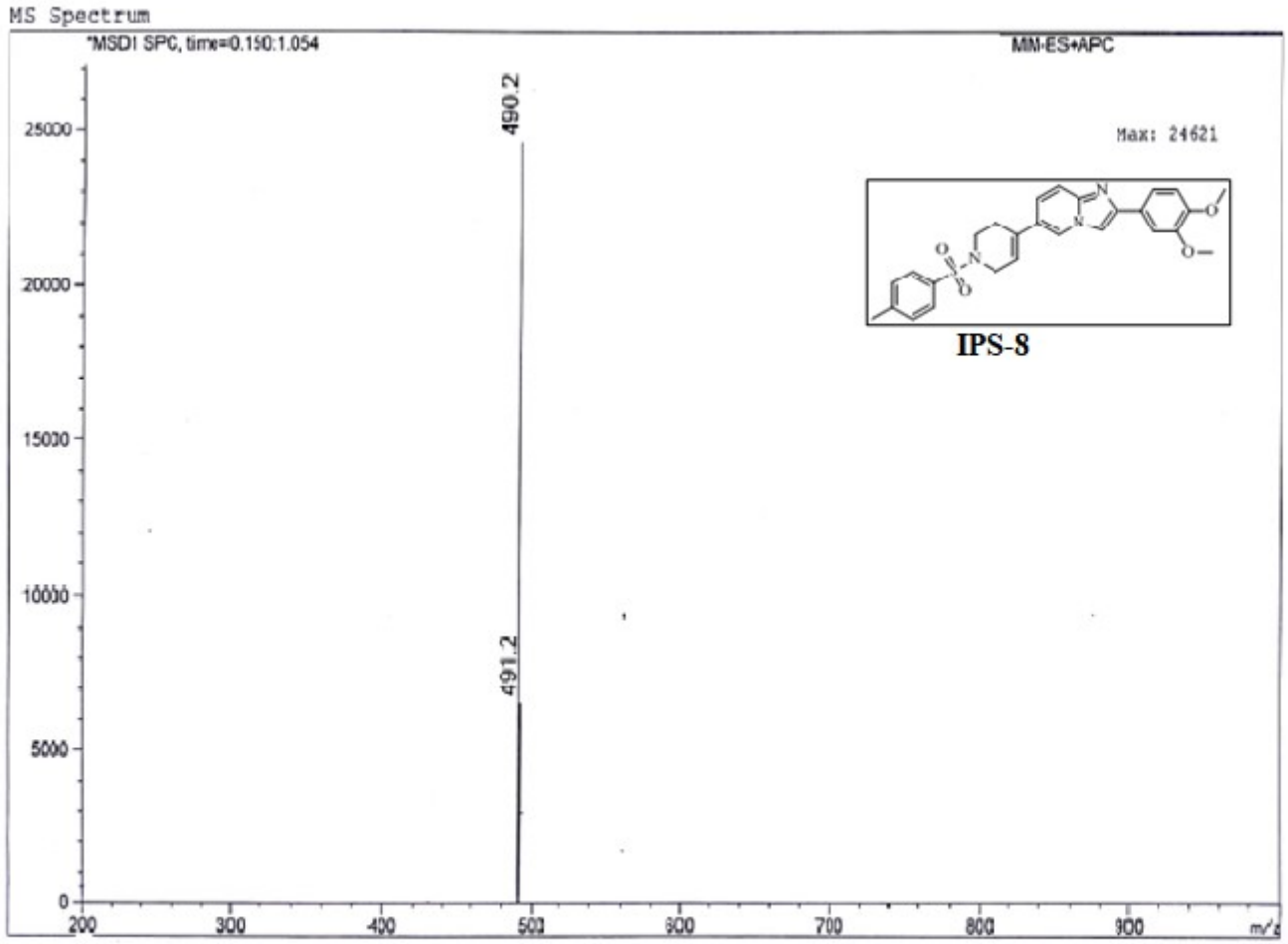

ESI MS spectrum of compound **IPS-8**

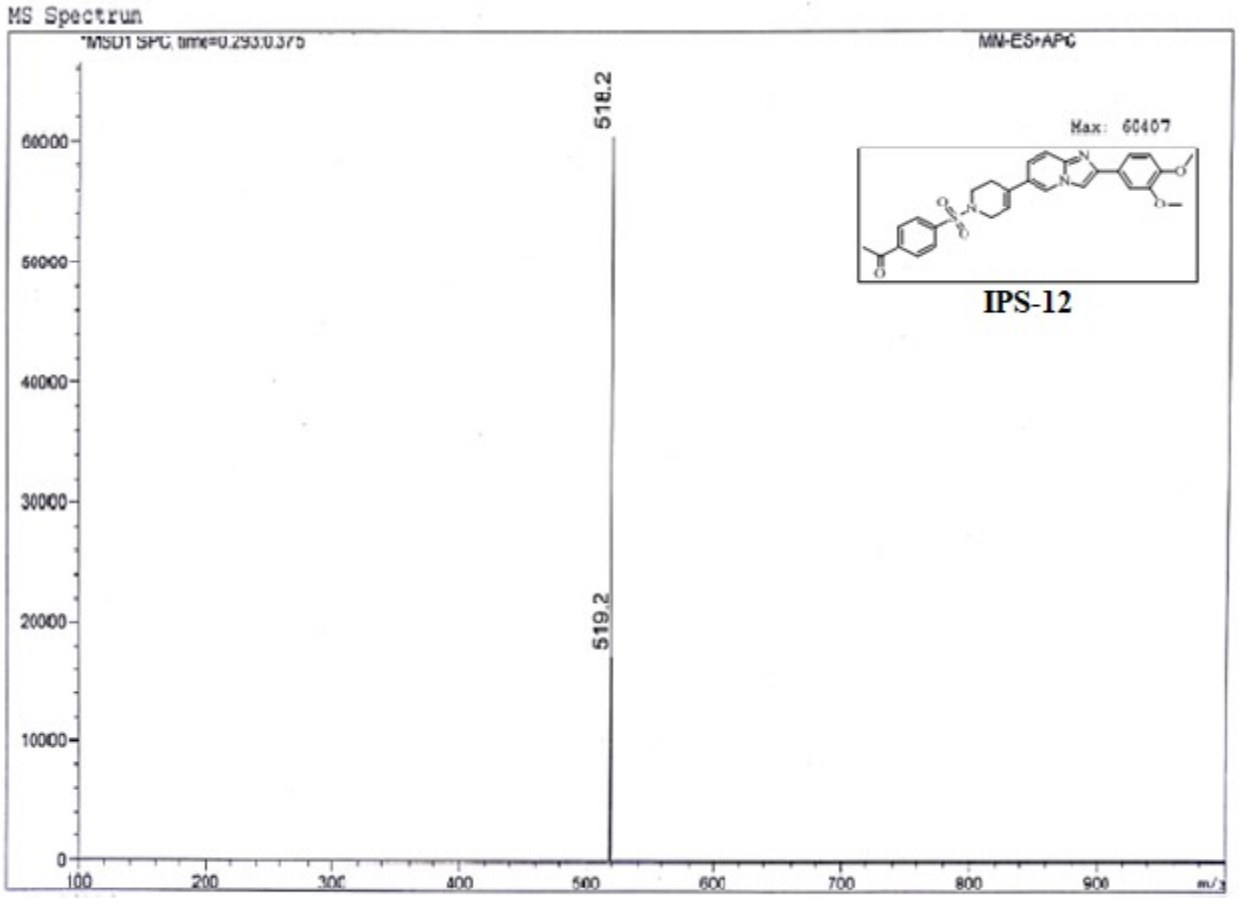

ESI MS spectrum of compound **IPS-12**

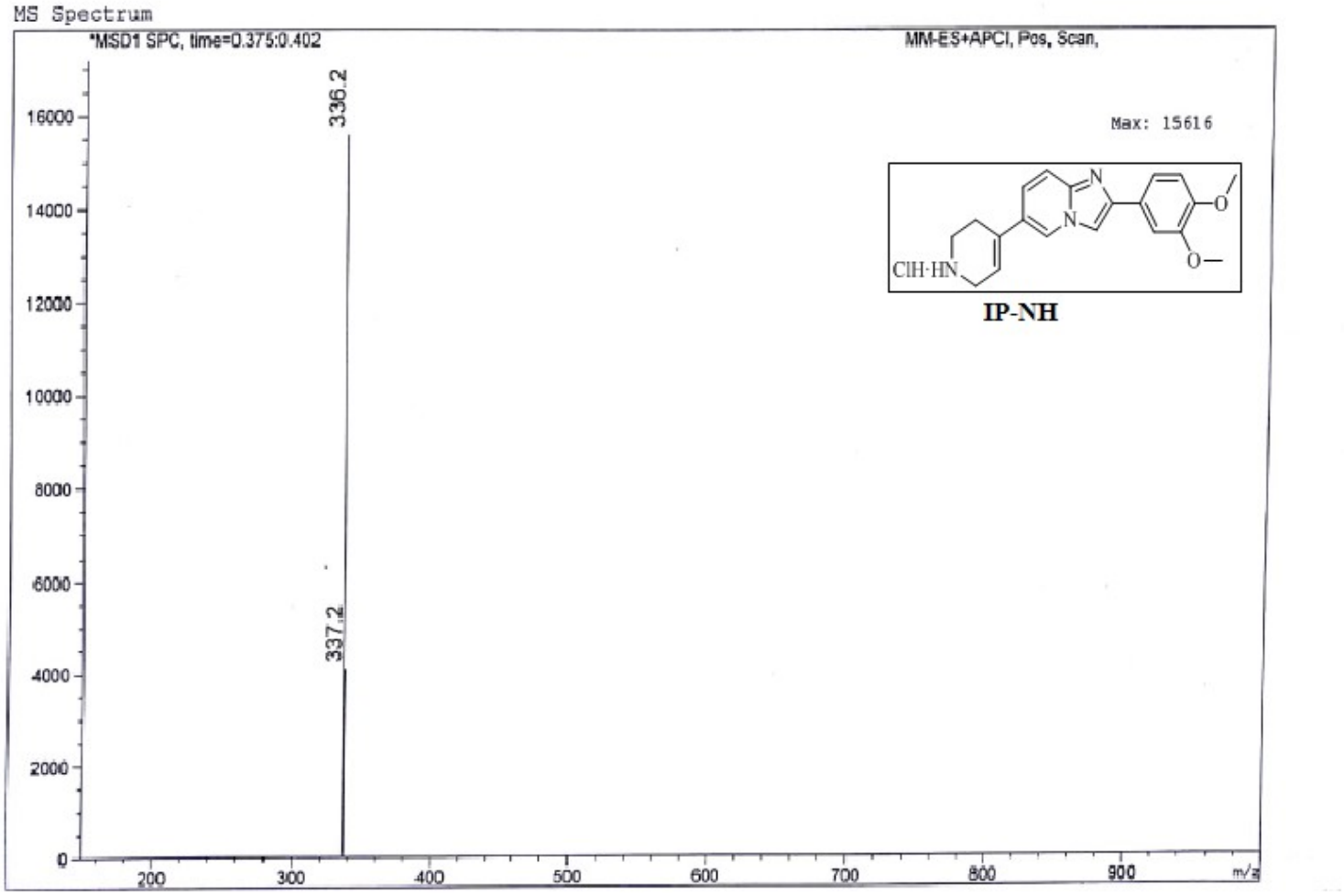

ESI MS spectrum of compound **IP-NH**

References:

1 Schrodinger, 2019-1. (n.d.). Schrödinger Release 2019-1: LigPrep, Schrödinger, LLC, New York, NY 2019.

2 S. K. Burley, H. M. Berman, C. Bhikadiy, C. Bi, L. Chen, L. Di Costanzo, and C. Zardecki, RCSB Protein Data Bank: biological macromolecular structures enabling research and education in fundamental biology, biomedicine, biotechnology and energy, *Nucleic Acids Res.,* 2019, **47,** D464-D474.

3 Schrödinger Release 2019-1: LigPrep, Schrödinger, LLC, New York, NY 2019 (n.d.).

4 Schrödinger Release 2019-1: LigPrep, Schrödinger, LLC, New York, NY 2019.

5 Schrödinger Release 2019-1: Schrödinger Suite 2019-1 Protein Preparation Wizard; Epik, Schrödinger, LLC, New York, NY, 2019. (n.d.).

6 Schrödinger Release 2020-4: Desmond Molecular Dynamics System, D. E. Shaw Research, New York, NY, 2020. Maestro-Desmond Interoperability Tools, Schrödinger, New York, NY 2020 (n.d.).

7 P., Mark, and L. Nilsson, Structure and dynamics of the TIP3P, SPC, and SPC/E water models at 298 K, *J. Phys. Chem. A.,* 2001, **105,** 9954-9960.

8 W. L. Jorgensen, D. S. Maxwell, and J. Tirado-Rives, Development and testing of the OPLS all-atom force field on conformational energetics and properties of organic liquids, *J. Am. Chem. Soc.,* 1996, **118,** 11225-11236.

9 D. A.Gibson, and E. A. Carter, Time-reversible multiple time scale ab initio molecular dynamics, *J. Phys. Chem.,* 1993, **97,** 13429-13434.

10 A., Cheng, and K. M. Merz, Application of the Nosé−Hoover Chain Algorithm to the Study of Protein Dynamics, J. Phys. Chem., 1996, **100,** 1927–1937.

11 G. Kalibaeva, M., Ferrario, and G. Ciccotti, Constant pressure-constant temperature molecular dynamics: a correct constrained NPT ensemble using the molecular virial, *Mol. Phys.,* 2003, **101,** 765-778.

12 B. Karan Kumar, Faheem, R. Balana Fouce, E. Melcon-Fernandez, Y. Perez-Pertejo Yolanda, R. M. Reguera, and S. Murugesan, Design, synthesis and evaluation of novel β-carboline ester analogues as potential anti-leishmanial agents, *J. Biomol. Struct. Dyn.,* 2021, 1-16.

13 B. K. Kumar, Faheem, K. V. G. C. Sekhar, R., Ojha, V. K. Prajapati, A. Pai, and S. Murugesan Pharmacophore based virtual screening, molecular docking, molecular dynamics and MM-GBSA approach for identification of prospective SARS-CoV-2 inhibitor from natural product databases*, J. Biomol. Struct. Dyn.,* 2020, 1-24.